A review of oil well cement alteration in CO2-rich environments

Bagheri, M., Shariatipour, S. M. & Ganjian, E.

Original citation & hyperlink:
Bagheri, M, Shariatipour, SM & Ganjian, E 2018, 'A review of oil well cement alteration in CO2-rich environments' Construction and Building Materials, vol 186, pp. 946–968.
https://dx.doi.org/10.1016/j.conbuildmat.2018.07.250

DOI 10.1016/j.conbuildmat.2018.07.250
ISSN 0950-0618
ESSN 1879-0526
Publisher: Elsevier

A review of oil well cement alteration in CO_2-rich environments

Mohammadreza Bagheri[a,*], Seyed M. Shariatipour[a], Eshmaiel Ganjian[b]

[a] *Flow Measurement and Fluid Mechanics Research Centre, Coventry University, Priory Street, Coventry CV1 5FB, UK*

[b] *School of Energy, Construction and Environment, Built & Natural Environment Research Centre, Coventry University, Coventry CV1 5FB, UK*

Abstract

The purpose of this study is to examine previous works undertaken that characterise the cement alteration due to its exposure to CO_2-bearing fluids attacking on the interfaces of cement-rock and cement-casing, or through cement cracks, and the cement matrix itself. Numerous studies have reported carbonation of well cements. The majority of studies reported self-healing behaviour of cements cracks observed under general CO_2 storage conditions. In addition, defective cement matrix and bonding between cement and casing were also found to be potential causes for leakage pathways. Albeit, severe conditions, such as high acidity degree of brine and high flow velocity, may negatively affect the self-healing behaviour of the cement.

Keywords: CO_2; Cement; Leakage; Geo-sequestration

1 Introduction

In the course of 132 years from 1880 to 2012, the average global combined land and ocean temperature has risen by 0.85 ℃ [1], a phenomenon now indelibly linked to anthropogenic greenhouse gas (GHG) emissions. Carbon dioxide is accountable for 9-26% of these GHG emissions [2,3]. One amelioration technique that can be adopted is the use of carbon capture and storage (CCS), which seeks to capture released CO_2 from power plants and subsequent injection of them into stable underground formations. Coal beds, aquifers, and depleted oil and gas reservoirs are of considerable interest for CCS. Amongst them depleted reservoirs are preferred since their structures have been well-characterised and studied over different periods of the reservoir's lifecycle. In addition, oil and gas reservoirs have maintained their integrity and prevent fluid permeation to the surface over millions of years, indicating their proven capability of storing fluids over a long duration. One additional benefit of CCS is that the CO_2 injection into oil and gas reservoirs is considered as an enhanced oil recovery strategy. One of the major problems with this type of projects is that quite a high number of abandoned wells have been cemented during the last century without meeting the necessary safe storage requirements. Drilled wells are the direct connection between underground formations and the surface. Any defects in the cement and plugs may later transform into potential leakage pathways. This is illustrated by a 30-year old cement core sample recovered from a CO_2-flooding site in West Texas. That demonstrated CO_2 leakage along the cement-shale and cement-casing interfaces, even though the cement retained its low permeability to prevent CO_2 flow [4]. Accordingly, an investigation of cement integrity exposed to CO_2-bearing fluids is of great importance for determining the probability of CO_2 leakage to the surface.

Carbon capture and storage (CCS) projects are designed to prevent large quantities of CO_2 from entering into the atmosphere. This will be done by effectively collecting CO_2 and transporting it from large

* Corresponding author.

Email address: bagherim@coventry.ac.uk

production point sources to storage sites where it can be deposited in underground formations and can remain there for thousands of years [5].

Typically, depleted oil and gas reservoir sites are the main subjects for CO_2 storage. The risk of CO_2 gas leakage to the surface from prior-drilled and abandoned wells can be assessed to speed up risk assessment [6]. It was also shown that wells which are drilled under an appropriate regulatory system for CO_2 and acid gas injection purpose are less probable to fail in comparison with other types of wells converted to injection wells [7]. Therefore, performing a robust drilling, completion, abandonment, and cementing under the supervision of reliable regulatory frameworks is vital to prevent CO_2 leakage. The cement used as well lining or plugs may have undergone an alteration process due to CO_2 exposure. This process may lead to either the aggravation or amelioration of leakage pathways depending on the conditions of the cement and the invading fluids [8].

The most potential leakage pathways within casing-cement-rock (rock can be a storage formation or caprock) assembly include the gap between rock and cement [9,10], the gap between the casing and cement [11,12], cracks in the cement [11,13–15] , and the cement matrix by itself [14,16–18]. CO_2 is injected generally in a supercritical form into underground formations [19]. In this state it has the physical properties of both a liquid and a gas which dissolves materials such as a liquid and can effuse through solids like a gas. The injected CO_2 dissolves in brine, as a ubiquitous element in depleted oil and gas reservoirs particularly around abandoned wellbores, results in carbonic acid formation [20]. CO_2-saturated brine with a pH lower than 4 starts moving through well cements due to diffusion or advection [21,22]. This movement brings the pore water within the unaltered cement with a pH more than 12.5 in contact with acidic brine [23]. This process leads to a reaction between the cement and brine leading to a gradual carbonation within the cement [12,24–29]. The continuous renewal of reacted CO_2-saturated brine at the cement interface accelerates the degradation of the cement and causes the depleted calcium region to be converted into an amorphous silica gel [27,29].

This paper provides a review of studies that have characterised the alteration in cement due to CO_2–bearing fluids attacking on the interfaces of cement-rock and cement-casing, or through cement cracks, and the cement matrix itself.

2 Characterisation of cement matrix alteration attacked by CO_2-bearing fluids

2.1 Involved chemical reactions

The dissolution of CO_2 in brine decreases its pH to below 4. The subsequent flow of this mixture through a carbonate formation leads to an increase of pH by 2. It is interesting to note that if the dissolution was to flow through a sandstone formation there seems to be a negligible impact on acidity [27]. Portland cement pore fluids normally have a pH between 13 and 14 [30], thereby exposing the cement to a CO_2-saturated brine reduces the pH of the pore fluids in the cement and triggers dissolution/precipitation reactions. To examine the impact of carbonated brine flow on well cements, class H cement pastes were exposed to a range of geo-sequestration temperatures and pH at a depth of 1 km [27]. The pre-equilibrium between calcium carbonate and the CO_2-brine solution showed no significant carbonated brine attack. Carbonic acid attacks the cement and results in carbonate which is then dissolved during the next phase. This reaction leads to a more porous silica gel. The governing equations are as follows [27]:

CO_2 dissociation

$$CO_2 + H_2O \leftrightarrow H_2CO_3(sum\ of\ H_2CO_3\ and\ dissolved\ CO_2) \leftrightarrow H^+ + HCO_3^- + CO_3^{2-} \quad \text{Eq. 1}$$

Cement carbonation

$$Ca(OH)_2(s) + 2H^+ + CO_3^{2-} \rightarrow CaCO_3(s) + 2H_2O \quad \text{Eq. 2}$$

$$C_{3.4} - S_2 - H_8(s) + 2H^+ + CO_3^{2-} \rightarrow CaCO_3(s) + SiO_xOH_x \quad \text{Eq. 3}$$

$$Ca(OH)_2(s) + H^+ + HCO_3^- \rightarrow CaCO_3(s) + 2H_2O \quad \text{Eq. 4}$$

$$C_{3.4} - S_2 - H_8(s) + H^+ + HCO_3^- \rightarrow CaCO_3(s) + SiO_xOH_x \quad \text{Eq. 5}$$

Calcium carbonate dissolution

$$CO_2 + H_2O + CaCO_3(s) \leftrightarrow Ca^{2+} + 2HCO_3^- \quad \text{Eq. 6}$$

$$2H^+ + CaCO_3(s) \leftrightarrow CO_2 + Ca^{2+} + H_2O \quad \text{Eq. 7}$$

SiO_xOH_x in Eq. 3 and Eq. 5 is an amorphous silica gel, and $C_{3.4}$-S_2-H_8 is calcium silicate hydrate (C-S-H) which is the binding phase of the cement paste with Ca/Si:1.7. These experiments were conducted under general conditions of 20 and 50 ℃ and CO_2 pressures of about 10 MPa. Effluent samples and pH measurements were taken twice a day during the first few days, and during subsequent phases performed every day. There was little alteration in the cement due to CO_2 exposure under pre-equilibrium with limestone. Accordingly, it seems that degradation in limestone or dolomite either occurred really slowly or did not occur at all.

Once the calcium carbonate precipitated, the brine was refreshed and the pH was lowered to below 5. Calcium carbonate then started to re-dissolve in the new CO_2-saturated brine brought in contact with the core cement [31]. It worth noting that the calcium leaching from C-S-H as the binding phase in cement do not limited just to the regions adjacent to the brine-cement interface. This process gradually begins from the calcium carbonate precipitation zone and increases towards the cement-brine interface. By decreasing the pH below 12, C-S-H dissolves incongruently [32], which leads to decline in the ratio of Ca/Si from around 2 to approximately 0.8 [23,33,34]. To simplify the modelling of the alteration in the cement, the C-S-H dissolution can be constrained to the silica gel zone due to the higher portlandite dissolution rate than that of C-S-H. Chasing any alterations in C-S-H during the reactions is difficult, because composing ions of C-S-H are not dissolved proportional to the stoichiometric coefficient. Therefore the composition of C-S-H varies along the process of dissolution. To simplify this problem, C-S-H is considered as a solid solution of hydrated silica gel and two fractions of portlandite. It is supposed that one of those portlandite fractions dissolves at the same rate of the free portlandite [33]. The solubility of the other fraction is assumed to be lower than free portlandite, and the remaining silica gel was considered to be insoluble. The evolution of C-S-H was modelled by considering an initial Ca/Si ratio steadily declassified to calcium carbonate and amorphous silica [32]. C-S-H was assumed as a composite of molar fractions of end-members of portlandite and amorphous silica [35,36]. It was shown that C-S-H dissolves incongruently at a high Ca/Si ratio and congruently by decreasing the ratio of Ca/Si. In the case of low Ca/Si ratio, the dissolution of C-S-H will be approximately equal to a tobermorite-like composition. Therefore, a rate law can be proposed for a description of C-S-H dissolution [34].

The solubility of CO_2 in brine decreases with increasing salinity and temperature, in contrast to the effect of enhancing pressure which improves CO_2 solubility [37,38]. When CO_2 is injected to depths more than 1 km, the local temperature is above the critical point of CO_2 (31 ℃) and high pressure of about 100 bars yields a density of 500 kg/m^3 [39]. The combined effect of pressure, temperature, and salinity on the penetration depth of CO_2-saturated brine into the cement is highly complex since the pH of the aqueous phase is a function of the composition of brine, cement, and host rock which are also affected by temperature and pressure [40,41].

2.2 Predominating phenomena

Generally, static conditions are preferred in many experiments [18,35,42–45]. The reason for this is based on the distance between the abandoned and injection wells, as at some distances from the injection well the CO_2-saturated brine moves extremely slowly that velocity can be neglected. Although, the connection between reservoirs and either overlaying layers or inside the well creates a pressure difference which enhances the velocity. Thereby, the advection phenomenon becomes important. Advection means movement of species contained in a fluid as a result of fluid bulk movement [46]. Different reasons may result in fluid movement such as pressure differential and thermal gradient. This phenomenon along cracks and gaps causes fluid flow which brings fresh CO_2-bearing fluids in contact with the cement

surface. Extremely low permeability porous mediums like cement with permeabilities typically far below 200 μD, practically remove advective flow from consideration within bulk matrix. Thus, their dominance can be restricted to the cracks and the gaps [26,31,47,48]. Nevertheless, reaction kinetics are considered to be faster than diffusion kinetics [49] which justifies the application of an adopting batch system for experiments [12,15,18,44,50].

The difference in concentration between the carbon/calcium species in CO_2-saturated brine and the unaltered cement zone encourages the diffusion of CO_2-saturated brine into, and the calcium-rich brine, out of the cement core. Static downhole conditions strengthen the assumption that the cement is altered by diffusion-dominated processes. Whereas advection may be supposed for the renewal of CO_2-saturated brine at the cement-brine interface [26,31,47,51,48]. However, the impact of advection, which is responsible for the renewal of CO_2-saturated brine at the interface between the cement and brine, is accounted by assuming a vertical motion of CO_2-saturated brine along any gaps [26,31,48].

A methodology for coupling the transport and geochemical modules of Dynaflow^{TM} [52] was derived to model mineral precipitation/dissolution, the aqueous phase speciation and the porosity dependant transport properties [26]. The CO_2 radial mass transfer was primarily responsible for cement degradation. The mass transfer in the vertical direction is mainly dominated by advection and in the radial direction by diffusion within the cement. The experiment design was based on the work of Duguid [53] by assuming constant fluid composition in the microannulus and considering radial diffusion as the major transport mechanism into the cement. Different parameters, such as the geometry of leakage pathways, boundary conditions, and chemical reactivity of the cement with CO_2 affect flow through cements and may result either in an opening-up or self-healing behaviour of the leakage pathways. To model this phenomena, the coupling geochemical aspect with transport aspect is inevitable. As reaction kinetics were assumed to be much faster than diffusion [49], the process was therefore assumed to be diffusion-limited, diffusion seen to be of great importance even for fluid flow through gas shale [54]. Two main non-linear equations were applied to describe equilibrium conditions coupled with the transport modulus using a sequential non-iterative approach (SNIA). The spatial distribution of the $CaCO_3$ polymorphs was examined using Raman microspectrometry and X-ray microdiffraction [43]. The fast reaction of the calcium-bearing phases in cement provides a convenient method for simulation since an assumption of the local equilibrium could be considered compared with diffusion into the cement. This assumption may sometimes be violated due to the formation of the metastable forms of the calcium carbonate. The presence of the three calcium carbonate polymorphs in the core that undergoes CO_2-rich fluid flooding signifies the importance of the kinetics over the presumed equilibrium. In fact, a local equilibrium for carbonation cannot be considered reasonably as long as metastable $CaCO_3$ polymorphs can be assumed to be present in the sample.

An experiment under static conditions was conducted by Kutchko et al. [55] illustrating a depth of penetration of about 1.68 mm and 1.00 mm for supercritical CO_2 and CO_2-saturated brine, respectively. Exposure of the cement to the supercritical CO_2 resulted in no evident separation zones. The length of diffusion showed a more linear behaviour with respect to the square root of time, a behaviour not seen when the cement was exposed to CO_2-saturated brine. The former observation follows the second law of Fick whereas the latter one was described using the Elovich equation [55].

2.3 Cement Durability

Barlet-Gouédard et al. [16] conducted an experiment under static conditions exposing the cement cores to the realistic downhole conditions of 90 ℃, 280 bars, and water with a pH of around 8 for durations ranging from a half-day to 3 months. It was demonstrated that Portland cement is sufficiently resistant to wet supercritical CO_2 or to CO_2-saturated water. The durability of cement is also a function of the curing process. For example, cement cured at 50 ℃ and 30.3 MPa is more resistant to carbonic acid attack compared with cement cured at 22 ℃ and 0.1 MPa, with a common curing time-of 28 days. The higher temperature and pressure are more representative of sequestration application conditions. In fact, a higher degree of hydration leads to a reduction in permeability and resistance to carbonic acid attack [25].

2.4 Formation of zones

Formation of different zones was confirmed during carbonation and degradation of cement. These four zones can be classified from the innermost part to the interface of CO_2-saturated brine and cement core as:

1) The unaltered zone.

2) The portlandite depleted zone.

3) The calcium carbonate precipitation zone.

4) The silica gel zone where the degradation occurs due to calcium leaching and C-S-H declassification.

Fig. *1* shows zones formed during carbonation and degradation processes [12,25,35,43,55]. Although, occasionally fronts are preferred for describing the alteration in the cement, the portlandite dissolution front, the carbonation and calcium carbonate dissolution fronts are widely used to indicate three main reaction fronts moving into the cement [15,18,56].

Two methods of mercury porosimetry and back-scattered electron (BSE) imaging were applied by Rimmelé et al. [18] to quantify the evolution of bulk porosity and local porosity gradients. The design of their experiment was similar to the work of Kutchko et al. [25]. It was confirmed that the carbonation front moves forward from the rims of the cement core into unaltered zones, even during the few first days of exposure. Mercury intrusion porosimetry (MIP) indicated a primary sealing stage corresponding to carbonation, followed by a dissolution phase. Local porosity gradients were produced using scanning electron microscope-BSE (SEM-BSE) image analysis and showed that during the first phases of attack, from day one to 3 weeks, the sealing stage was active and responsible for decreasing the porosity of inner part of the sample, while in the next phase the carbonation front was no longer visible and had reached the centre of the sample. During this period, porosity increased as a result of the recently formed calcium carbonate undergoing dissolution. Porosity in the cement zones illustrated an immediate high increase in the cement-brine interface due to the dissolution of calcite. Within the next region, calcite precipitation led to a decreased porosity area, towards interior parts of the sample. In the simulation, porosity was again seen to be enhanced as a result of calcium leaching to produce Ca^{2+}. Parallel permeability (permeability of casing-cement-rock assembly when the flow direction is parallel to the interfaces between them) is more important, however, if the bonding between formation and cement is of good quality an increase in parallel permeability will not impact the leakage. Indeed, permeability can be divided into two types depending on the direction of diffusion with respect to flow direction to simulate wellbore cement alteration [45]. The direction of diffusion and flow are the same for transverse permeability and the flow direction is vertical to the diffusion direction for parallel permeability.

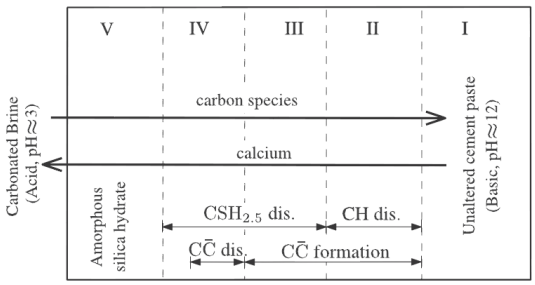

Fig. 1: Formation of different zones in a cement exposed to CO_2-bearing fluids showing five zones from the right to the left side including: unaltered zone (I); portlandite dissolution zone(II) in which calcium carbonate ($C\bar{C}$) precipitation also simultaneously occurs; zone (III) accounted for the start of C-S-H (in this case $CSH_{2.5}$) dissolution and gradual termination of $C\bar{C}$ precipitation; zone(IV) dominated by C-S-H and $C\bar{C}$ dissolution, and; amorphous silica gel zone(V) depleted from calcium content to a great extent immediate to the brine-cement interface [33].

2.5 Depth of reaction fronts

The initial properties of the cement affect its evolution. For example, a high ratio of initial portlandite to porosity produces local sharp calcite zones which reduces the diffusion of CO_2-saturated brine into the cement and intensifies the deterioration rate in the zones close to the cement-brine interface. Low-portlandite and high porosity cement types are not typically clogged. Furthermore in this case the depth of penetration is generally higher than for cements with a high-portlandite and low-porosity content [8,57,58]. A reactive transport model was developed by Brunet et al. [57] to account for the alteration of cement in contact with CO_2-saturated brine under diffusion-controlled conditions. Three main aspects incorporated in the modelling approach included the coupling of the reaction thermodynamics and kinetics with the transport processes, the impact of initial cement properties, and the connection between changes within the cement composition to long-term flow transport properties. This analysis raised the cementation factor as the most critical parameter that controls the dynamics of the cement-CO_2 system. Observations illustrated that no clogging resulted from low-portlandite and high-porosity cement, while clogging was observed for high-portlandite and low-porosity conditions. Over the course of 200 days, different ratios of portlandite to porosity simulations showed there to be from less than 1 mm to around 6 mm depth of penetration .

Cement samples retrieved from a well exposed to natural gas CO_2 to assess the degree of carbonation corresponding to the CO_2 dissolved in the pore water of surrounding formation indicated that a carbonation depth of millimetres to centimetres is expected, even in the absence of any cracks or annular gaps [59]. Sauki and Irawan [60] exposed class G cement to supercritical CO_2 for a period of 120 hours at two temperatures, 120 and 40 ℃, showed a penetration depth of 0.78 and 0.55 mm, respectively. Samples exposed to either CO_2-saturated brine or wet supercritical CO_2 for 120 hours identified four main zones including an innermost unaltered zone, a depleted in portlandite zone with a thickness of 50-100 μm, a 100-200-μm zone with a high calcium content, and an outermost zone with a thickness of 200-400 μm.

2.6 Impact of additives

Typically, pozzolans are used in cement to reduce the overall cost of cementation and reduce the density of the slurry. It was predicted that CO_2-saturated brine and supercritical CO_2 will penetrate to a depth of around 170-180 mm in pozzolanic-cement with the volume fraction of 35:65 over a period of 30 years, confirming that the rate of penetration increases with the introduction of pozzolan-amended cement [44]. It was observed that the reaction of pozzolanic cement paste was remarkably faster than neat cement with CO_2, although any degradation of physical properties was not noticeable in pozzolanic cement paste [61]. Their findings indicated that the rate of penetration in pozzolanic-amended cement is higher than in neat cement. Pozzolan additives increase porosity, cause a higher rate of diffusion, and reduce the portlandite content. Thereby, they prevent the high precipitation of carbonates, that positively influences the penetration of CO_2-bearing fluids into the cement [23]. These studies indicate a further need for investigating the impact of the other types of additives affecting cement behaviour.

2.7 Modelling

Cement alteration modelling is highly advantageous for extrapolating short-time scale experiment studies. In addition, performing a sensitivity analysis concerning a determination of the variables controlling an alteration in the cement is expensive [45], which makes modelling more feasible.

A diffusion-reaction model was developed by Liaudat et al. [33] to regenerate experimental data of Duguid and Scherer [27]. To simplify modelling, reactions corresponding to aluminium, iron, and sulphur (solid and aqueous) species were removed from consideration. On the other hand, modelling the C-S-H progress during reactions is difficult, since composing ions composed of C-S-H are not dissolved proportional to the stoichiometric coefficient. Therefore the composition of C-S-H varies along the process of dissolution. It was claimed that front penetration only can be addressed by involving the growth of effective diffusivity of the material because of degradation. Moreover, kinetics' constants are also highly determinant in specifying the width of the degradation front. The proposed quantitative reactive-transport model used four primary species; including calcium, total carbon, chloride, and alkalis.

Calcium and total carbon were based on diffusion-reaction equations and chloride and alkalis (sodium and potassium) which were defined only by diffusion. This model, although is relatively simple, successfully predicted the experimental data obtained from the study of Duguid and Scherer [27]. To predict cement degradation over thousands of years, typical of carbon sequestration, a voltage across the cementitious material was applied. This method simulated the fast degradation of the cement in time-order of an experiment for depicting procedure over long timescales [62]. This process was dominated by the forced transport of the ionic species, and diffusion was slower than envisaged.

2.8 Conducted experiments for characterising of cement matrix alteration

Table *1* provides information regarding experiments which have been conducted to investigate impact of CO_2-bearing fluids on the cement matrix.

Paper	Curing conditions	Method of experiment	Applied temperature condition	Applied pressure condition	Core dimension	Properties of fluid	Time-length of experiment	comment
[43]	• Class G cement • Cores cured for 72 hrs at 90 ℃ and stored in water.	Batch system	90 ℃	30 MPa	• Diameter: 30 mm • Length: 65 mm	• pH of CO_2 saturated water: 2.9 • Calcium content: 80 mg/litre	3, 22, 35,and 51 days	• This work focused on the forming metastable calcium carbonates ahead of reaction front. • The Simulation predicted a depth of around 1.1 mm for the movement of carbonation front into the cement during 84 hrs.
[62]	Class G cement	The leaching is induced by a forced transport in CO_2-rich environment (LIFTCO2) procedure.	From ambient temperature to 50 °C	1 atm	• Diameter: 5 cm • Length: 2.5 cm	N/A	4 days, 5 weeks	• The long-term degradation was simulated using an electrophoresis voltage between 10-50 V • The voltage difference was used to accelerate the reaction process to model long-term durability of cement. • The depth of altered zone after 5 weeks at the cathode side: 800 µm, and at the anode side: 200 µm.
[45]	Curing time: 28 days	Batch system	50 °C	150 bars	• Diameter: 12 mm • Length: 60 mm	• Initial pH: 2.9 • Brine salinity: 1 wt % NaCl	2.5, 28, and 90 days	• The co-injection of H_2S and CO_2 in a cement with 35 vol % pozzolan and 65 vol % class H Portland cement was investigated. • The simulation showed a calcite peak at 0.4-mm depth after 90 days.
[55]	• Class H neat cement. • (water to cement ratio) W/C: 0.38 • Cement moulds were submerged in a 1 wt % NaCl (brine) • Temperature: 50 °C • Pressure: 30.3 MPa • Samples were demoulded from casts after 3 days and hydrated for of 28 days	Batch system	50 °C	30.3 MPa	N/A	• Initial pH: 2.9 • Brine salinity: 1 wt % NaCl	Up to one year	The extrapolation indicates a penetration depth of 1.68 ±0.24 mm for the supercritical CO_2 and 1.00 ±0.07 mm for the CO_2-saturated brine after 30 years.

[44]	• Class H cement • 35:65 and 65:35 (volume ratio of pozzolan to cement) pozzolanic cement blend • Temperature: 50 °C • Pressure: 15 MPa • Curing time: 28 days	Static condition	50 °C	15 MPa	• Diameter: 12 mm • Length: 130 mm	Fresh water	5, 7, 9, 14, and 31 days	• The effect of pozzolan additives was considered. • Penetration depth into 35:65 pozzolan-cement blend Class H: 170-180 mm under the CO_2-saturated brine and supercritical CO_2 conditions over 30 years • The system 65:35 pozzolan-cement blend class H fully reacted with supercritical CO_2 within 2 days: 5 mm in 2 days under CO_2-rich brine conditions, however, it was not possible to precisely determine an alteration rate for this system.
[61]	• Class H cement • 35:65 and 65:35 (volume ratio of pozzolan to cement) pozzolanic cement blend • Curing time length: 28 days • Samples were submerged in 1 wt % NaCl • Pressure: 2200 psi • Temperature: 50 °C	Batch system	50 °C	2200 psi	Diameter: 2 inch	Brine salinity: 1 wt % NaCl	31 days	It was found that reaction of pozzolanic cement paste is remarkably faster than with neat cement, although degradation of physical properties is not significant in pozzolanic cement paste.
[27]	• Class H neat cement • W/C: 0.38 • Cement moulds were submerged in a 0.5 M NaCl • Temperature: 20 ℃, 50 ℃ • Curing time: 12 months	Flow-through reactor Continuously stirred	20, and 50 ℃	Atmospheric pressure	• Diameter: 7.5 mm • Length: 200 mm	• pH: 2.4, 3.7 • Brine salinity: 0.5 M NaCl	Up to 30 days	• The brine was renewed in contact with cement. • The Rate of penetration front movement: 0.025-0.240 mm/day for neat paste samples under sandstone-like conditions and 0.023-0.444 mm/day for the paste containing 6% bentonite under sandstone-like conditions • No apparent damage over the course of the experiment • Time-length:~ 1 month
[63]	• Class G cement • W/C: ~ 0.40 • Pressure: 138, 296, and 345 bars • Temperature: 50, 74, and 83 ℃ • Setting time: 24 hrs • Antifoam-class G cement or a 50:50 mixture of cement class G and pozzolan	N/A	N/A	N/A	• Diameter: ~ 37 mm • Length: ~ 27 mm	N/A	It was supposed for a time-length of 1 to 9 months of experiment	• It was aimed at investigation of different curing conditions on the permeability evolution
[16]	• Class G cement with an antifoam agent, a dispersant and a retarder • Curing time: 72 hrs • Pressure: 207 bars • Temperature: 90 ℃	Static condition	90 °C	280 bars	• Diameter: 1.27 cm • Length: 2.54, 5.08 cm	• Fresh water • Expected pH resulted from dissolution of CO_2 in water: 2.8 to 3	Half-day, 2, 4 days, 6 weeks, and 3 months	• Portland cement is not sufficiently resistant to wet-supercritical CO_2 or to CO_2-saturated water • Depth of penetration: 1-2 mm after 44 hrs; 5-6 mm after 3 weeks; and ~ 7 mm after 6 weeks

[18]	• Class G cement • Curing time: 72 hrs • Pressure: 207 bars • Temperature: 90 ℃	Static condition	90 ℃	280 bars	• Diameter: 1.25 cm • Length: 2.5, 5 cm	Fresh water	Half-day, 2, 4 days, 6 weeks, and 3 and 6 months	Depth of penetration: 0.5-1 mm after half a day; 1-2 mm after 2 days; 5-6 mm after 3 weeks; and ~7 mm after 6 weeks
[25]	• Class H Portland cement • W/C: 0.38 • Four types of curing conditions: 1- 22 ℃ and 0.1 MPa; 2- 22 ℃ and 30.3 MPa; 3- 50 ℃ and 0.1 MPa; 4- 50 ℃ and 30.3 MPa • Curing time: 28 days • Cement moulds were submerged in 1 wt % NaCl	Static condition	50 ℃	30.3 MPa	• Diameter: 12 mm • Length: 130 mm	Brine Salinity: 1 wt % NaCl	9 days	• The cement cured at 50℃ and 30.3 MPa was more resistant to carbonic acid attack rather than cement cured at 22℃ and 0.1 MPa. • Depth of reaction front penetration: 0.22-0.59 mm over the course of 9 days.
[60]	• Class G cement • W/C: 0.44 • Curing time: 8 hrs • Curing condition: (140 bars and 40 ℃), (140 bars and 120 ℃), (105 bars and 40 ℃)	Static condition	40, and 120 ℃	105, and 140 bars	• Diameter: 1.5 inch • Length: 2 inch	Brine Salinity: 0.01 M NaCl	24, 72, and 120 hrs	It was confirmed that formation of $CaCO_3$ may increase the compressive strength

Table 1: Experimental setup used by different authors to analyse cement alteration due to contact with CO_2-bearing fluids

3 Effect of cracks on the rate of cement alteration

3.1 Predominating Phenomena

The safe, reliable, and long-term underground CO_2 storage justifies exploring sound strategies for the assessment of CO_2 leakage to the surface. One of the possible leakage source of CO_2 to the surface occurs through damaged well cements. Mechanical constraints are one of the main sources for irreversible cement damage. Experiments based on batch systems are not able to regenerate the combined impact of chemical and hydrodynamical processes where reactants are renewed continuously and diffusion is the main transport mechanism [64]. Generally, the permeation of CO_2-saturated brine into the cement was assumed to be dominated by diffusion [8,26,31,48]. Advective transport was also considered along the interface between the fracture and brine.

Experiments were conducted under either a constant pressure differential or constant flow rate. A constant pressure differential is more likely to occur in downhole conditions of abandoned wells rather than at a constant flow rate. Although, longer cores are required for investigating cement alteration under a constant pressure gradient in order to allow longer residence time, using this method increases the precision of small changes in conductivity because of precipitation on the surface of the fracture [8,48,65,66]. Nonetheless, constant flow rate conditions were also extensively applied to examine cement alteration [14,29,67]. Flow-through experiments renew the CO_2-saturated brine that is in contact with fracture surface, thereby exacerbating the degradation process. This condition is likely to occur when a direct connection between the storage formation and overlaying layers, above caprock, is formed.

The stability of a defect is influenced by both mechanical and chemical phenomena, even when compressibility and elasticity are negligible. The combination of the reaction and flow through the defect may trigger a width reduction downstream due to calcite precipitation, while upstream, the silica gel is formed and leached from the calcium [13].

Typically, cement matrix permeability is lower than 200 μD [44], as a standard maximum permeability recommended by American Petroleum Institute (API). Therefore unless in the case of a high degree of cement carbonation and degradation, the cement matrix alone may not be particularly prone to leakage in the presence of fractures, microannulus, and channels. These conduits are the most potential leakage pathways based on, generally, a large difference in permeability between them and the cement matrix. Tortuosity and roughness can reduce the predicted permeability, predicted by theory of smooth parallel plate cracks, by a factor of 4 to 6 [68]. The cement permeability is extremely low and fracture can be assumed to be the dominant flow path that is highly affected by the cement reactions. Huerta et al. [14] showed that the leakage of CO_2-rich fluids along a wellbore may restrict the leakage pathway in the case of a small initial aperture and the sufficient residence time is allowing for the mobilisation and precipitation of minerals along the fracture.

Mainguy and Ulm [24] investigated the coupled diffusion-dissolution process in a reactive porous media detached by a fracture channel. They provide a framework for formulating diffusion-dissolution behaviour of reactive transport porous media by assuming convective transport to be negligible in comparison with solute diffusion. The role of convective transport typically becomes important in the presence of a high-pressure gradient and/or fast fluid flow across a porous media whereas for microcracks and non-smooth cracks diffusion is the governing force. Solute evacuation from small crack openings gradually slows down over a long time. The length of diffusion in the fracture is appropriate to the quadratic root of time. While the square root of time describes dependency of the length of diffusion into the bulk material to time in one-dimensional degradation. Their finding disclosed that the propagation of the dissolution front, and in the general chemical degradation of porous material, does not significantly increase due to a small crack.

Diffusion was assumed to dominate the transport of CO_2-rich solution into fractured marl cores (as a caprock) [69]. Computed outlet concentrations at low flow rates match reasonably with the experiment results, while at a higher flow rate they did not match precisely. Nevertheless, most of the dissolution patterns were reproduced in their simulation. It was shown that the calcite dissolution rate at the interface of the fracture and rock matrix was faster than the internal parts of the matrix, due to the direct contact of advective flow with calcite. In fact, by forming new altered zones within matrix, the contact surface area of the calcite and solution decreases and partaking minerals alter, thereby impacting the alteration process [57,70].

Iyer et al. [15] discussed the effect of the relative rates of reaction and diffusion on the precipitation of calcium carbonate within narrow leakage pathways in cement. The model in [10,29,71] was developed to incorporate the reaction-rate limited behaviour of the front movement. Actually, the previous model had a limiting assumption that reactions occur at rates much faster than the rate of diffusion, while in the situation where fronts are close to each other diffusion is faster than the reaction rate. By developing this model they studied the changes in permeability due to reaction-limited conditions, the implication of calcite precipitation and mechanical deformation on fracture sealing, and the reason for the different behaviour of cements that were subjected to previous calcium leaching. Applying the reaction-limited model and coupling it with an appropriate mechanical deformation model made it possible to account for fracture sealing attributed to precipitation, chemical and mechanical changes. Although it was confirmed that mechanical deformation may not solely be responsible for fracture sealing, at the same time it might intensify the effect of chemical sealing.

The fracture aperture decreases in areas with low aperture due to calcite precipitation while the preferential pathways are extended where the apertures of higher values are present. The rate of degradation decreases as a consequence of the distance formed between the reaction fronts and fracture where reactants are renewed by advection [47]. In this work, the amorphous silica layer was modelled and the effect of fracture aperture heterogeneity was accounted-for in the clogging mechanism. Fracture patterns follow the initial heterogeneity and initial distribution of aperture along the fracture that firmly

controls probable leakage. Self-healing behaviour was expected to occur in low aperture zones, while perennial, localised flow most likely occur in highly connected aperture paths.

3.2 Effect of residence time

Cao et al. [66] presented a reactive transport model aimed to investigate the property evolution of fractured cements. In this model a threshold was proposed to identify the fracture opening from self-sealing behaviour. This behaviour is likely to occur in low initial fracture apertures. Residence time played a significant role in their modelling. It was shown by increasing residence time precipitation became the dominant process leading to fracture sealing. Whereas permeability illustrated an increase in decreased residence times. Fast flow rate and the abundance of CO_2 reduces the probability of self-sealing behaviour, while increasing the residence time allows the precipitation process to clog leaky wells [48].

Fast flow to some degree prevents a permeability change and tends to keep the aperture open. A low flow rate may cause calcium carbonate precipitation and lead to self-sealing. A sensitivity analysis showed that, at the beginning of sealing, changes in the specific area of portlandite had the largest effect [8]. Increasing both portlandite and calcite have the same impact on the initiation of sealing. On the other hand, a higher matrix flow resulted from a higher matrix permeability, contributing to faster fracture sealing due to sharper calcite peak. A higher fracture/matrix permeability ratio produces a reduction in calcium concentration leading to a less dense calcium carbonate precipitation zone. For exceedingly low flow rate, it was shown that fracture permeability declines, while at a high flow rate the permeability remains rather constant. In addition, in the case of an intermediate flow rate, the hydraulic aperture could increase [64].

Generally, a high flow rate brings a huge amount of unreacted or fresh acidic brine in contact with the fracture surface which aggravates the leaching of minerals from fractured cement wells and leads to the opening [8,58,66]. A fracture opening increases permeability and, if pressure gradient remains constant, this process results in a higher flow rate through the fracture. In fact, a positive cycle is created thereby increasing permeability. In low flow rate conditions, however, calcium carbonate has enough time to precipitate at downstream positions which seals the fractures. The concept of residence time on the characterisation of fracture behaviour, self-sealing or opening, as the ratio of the fracture volume over the flow rate was stated which determines a threshold for separating these two behaviours [8,14,48,58,66]. Increasing residence time enhances the opportunity for leached minerals from the cement at the inlet in supersaturated influent to deposit downstream, and leading to self-healing behaviour. For low residence time range, leached minerals will be depleted from the fracture without having sufficient time to deposit at downstream locations, therefore the fracture aperture starts to increase. Despite statements in [8,48,66] disclosing the residence time threshold as a criterion to separate self-healing from fracture opening behaviour, many studies indicated that self-healing behaviour is more likely to occur at normal conditions of underground carbon storage [13,14,29,47,48,64,69,72–74].

3.3 Mechanical behaviour of cracks

The assumption of plastic behaviour and deformation of cement under stress to block the leakage pathway was speculated by Huerta et al. [72]. A characteristic dependence was found between fracture aperture change and confining stress for unreacted fractured cores. A moderate reaction of fracture with a low pH brine resulted in the aperture alteration twice as high for the same change in the confining pressure in the unreacted fracture due to loss of mechanical strength on the fracture surface. The developed reaction of fracture with low pH brine leads to significant plastic defamation and reduces the confining pressure to its initial value. The mechanical weakening of the cement core due to reaction causes a fast closure of the aperture with increasing confining stress. Furthermore, the joined degradation of the cement with decreasing fluid pressure could also result in self-healing behaviour of wellbore cements [73].

The K (bulk modulus), G (shear modulus) moduli, and the elastic wave velocities of the annular carbonated samples depicted a high degree of sensitivity to confining pressure, up to 15 MPa. That is interpreted as the elastic closure of micro-cracks [75]. Performing a sensitivity analysis on the

experiments is time-consuming and expensive, therefore simulations are preferred. At the beginning of sealing, changes in the specific area of the portlandite have had the largest effects on the start of sealing, indicated by sensitivity analysis conducted in [8].

3.4 Formation of zones

At the inlet of core cement, in flow-through experiments, zone formation is generally more distinct than downstream locations along the fracture length. Gradually, by closing the outlet, these zones become narrower, and depending on the residence time, calcium carbonate precipitation begins at a position in the fracture length where fluid within the fracture becomes supersaturated with the concentration of calcium content. If this assumed position is beyond the core length then the occurrence of fracture opening will be more probable, otherwise these process are likely to yield self-sealing [15,76].

3.5 Conducted experiments for investigating effect of cracks on the rate of cement alteration

Table *2* summarises information of experiments which have been conducted to explore mutual effects of cement degradation on flow through cracks and vice versa.

Paper	Curing conditions	Method of experiment	Applied temperature condition	Applied pressure condition	Core dimension	Properties of fluid	Fluid rate/ pressure gradient	Aperture	Time-length of experiment	comment
[14]	• Class H neat oil well cement • W/C=0.38 • Curing procedure: samples were cured under temperature of 50 ℃ and ambient pressure for the first 3 days and then removed from moulds and submerged in water at ambient temperature and pressure for next 28 days.	Flow-through	N/A	Confining pressure: around 500 psi	• Diameter: 2.54 cm • Length: 3.19-7.17 cm	• Injection pH: 2-3.15 • Hydrochloric acid was used as an analogue of CO_2-rich fluids to decline experiment time scale	Flow rate: 0.1-12 mL/min	Initial hydraulic aperture: 24-122 μm	Total fracture volume injected:1029-101714	The solubility of cement increases as pH declines, in consequence, cations are freed (e.g., Ca, Al, Fe) and precipitation resulted from mixing aqueous phase cations with high pH pore fluid ahead of the acid front. Their experiments mostly follow this trend to highlight behavioural key types rather than reproducing precise downhole conditions.
[64]	• A sulphate-high resistant Portland cement (SRPC) • W/C: 0.4 • Curing time: 4 months	Flow through	60 ±0.5 ℃	Pore pressure: 10 ±0.1 MPa	• Diameter: 9 mm • Length: 18 mm	• Entry brine composition: 0.5 M NaCl and 0.053 M $CaCl_2$ • pH of entry brine: 3.45	• Name of fractured samples: P1, P2, and P3 • Constant flow rate: for P1: 2 mL/min; for P2: 0.2 mL/min	Fracture aperture; 5 (P3), 25 (P2), and 35 μm (P1) using micrometric gauge sheet	For P1: 5.5 hrs; for P2: 50 hrs	The detected zones for experiment duration of 5.5 hrs: (i) a high porosity zone of around 100- micron-large; (ii) a dense zone with very low porosity of around 100 microns; (iii) a zone with higher porosity than the second one but lower than the first one of around 50 microns and (iv) the non-reacted cement; for experiment duration of 50 hrs, the same zones were identified except the first one, and thickness of third zones is around 450 microns.
[66]	• Class H ordinary Portland cement • W/C = 0.38 • The cement moulds are submerged in 1 wt% NaCl • Curing time: 72 hrs • Pressure: 8.936 MPa • Temperature: 50 ℃ • Curing time length: 28 days	Flow-through	25 ℃	Confining pressure: 6.343 MPa	• Diameter: 37.2 mm • Length: 77.2 mm	• Brine salinity: 1 wt% NaCl • Average pH of CO_2-saturated brine before core flooding: 3.9	Flow rate: 0.008 cm^3/s	212 μm obtained from computed tomography (CT) images	190 hrs	• Three cores were stacked together and build a length of 224.8 mm • Thickness of reaction zones at inlet after 190 hrs from fracture interface towards interior parts of cement: (zone 1, high loss of calcium, ~ 300 µm); (zone 2, precipitation of calcium carbonate, ~ 200 µm); (zone 3, portlandite depleted zone, ~ 150 µm)
[47]	• Cement class G • W/C = 0.4 • The slurry, firstly, was cured for 24 hrs at temperature of 50 ℃, then placed in a PVC mould for duration of four months to reach maximum hydration	Flow-through	60 ℃	10 MPa	• Diameter: 9 mm • Length: 18 mm	Brine salinity: 0.5 M NaCl and $7.1*10^{-4}$ $CaCl_2$	• The experiment have been conducted under constant flow conditions • Constant flow rate: 100 μL/min, corresponding pressure gradient: 0.5-1 MPa/m	The mechanical aperture before experiment was about 14 μm which was in reasonable agreement with hydraulic aperture	100 hrs	Depth of penetration of reaction front during 100 hrs: up to around 1.3 mm
[73]	• Cement class H • Curing at temperature of 125 ℉ and under atmospheric pressure	Flow-through	N/A	Loading cycle of increasing confining pressure to maximum of typically 750 psia	• Diameter: ~ 2.5 cm • Length: ~ 5 cm	CO_2-saturated brine	Flow rate: 0.01-10 mL/min	Fracture aperture was measured as a function of confining pressures ranges from 10 μm to 22 μm	7 and 12 days	The joined degradation of cement with decreasing fluid pressure can result in self-healing behaviour of wellbore cements

[48]	• Cement class H • W/C= 0.38 • Samples, firstly, was cured for 3 days at temperature of 50 ℃ and under ambient pressure, then placed in deionised water for during of 28 days at the same temperature and pressure	Flow-through	Around 22 ℃	• For constant pressure gradient experiment: Confining pressure: 1896-2457 psi Pressure differential: 2.0-55.1 psi Flow rate: 0.006-0.13 mL/min • For constant flow rate experiment: Confining pressure: 1519-1653 psi Flow rate:0.25-3 mL/min Pressure differential: 0.2-5.7 psi	• For constant pressure gradient experiment: Diameter: 2.54 cm Length: 21.9-24.38 cm • For constant flow rate experiment: Diameter: 2.54 cm Length: 5.37-7.24 cm	CO_2-saturated distilled water	N/A	• For constant pressure gradient experiment: Hydraulic aperture: 3-17 μm • For constant flow rate experiment: Hydraulic aperture: 33-47 μm	• For constant pressure gradient experiment: Total volume injected to seal: 1.172-6.51 mL • For constant flow rate experiment: Total time: 477-3034 min	Residence times were in the range of 48-360 s for constant pressure gradient conditions, while for constant flow rate were much lower from 1 to 21 s

Table 2: Experimental setup used by different authors to analyse cement alteration in the presence of cracks due to contact with CO_2-bearing fluids

4 Effects of gap between the casing and cement on the rate of cement alteration

Bachu and Bennion [11] carried out two experiments to investigate CO_2 leakage through well cements. Their work was categorised into two main sections; including, a geochemical analysis of CO_2 leakage, and probing effects of radial cracks in cement and annular space between the wellbore casing and cements. A good quality cement with a permeability of 0.1 μD was subjected to 90 days of CO_2-saturated brine at in situ conditions. During the first phase of their project the permeability declined promptly. The rapid fall could be attributed to the formation of a carbonate material layer in contact with the cement and CO_2-saturated brine, which prevents further cement degradation. Moreover, CO_2 exclusion led to multiphase flow and relative-permeability effects which decreased permeability. However, it is possible that very fine particles freed due to the carbonation process caused plugging and reducing permeability. A good quality bonding between cements, casing and surrounding rock is a reliable barrier to upward CO_2 movement, though an aperture of 0.01 to 0.3 mm might lead to a remarkable enhancement of at least six orders of magnitude in permeability.

Carey et al. [12] proposed that an enormous amount of CO_2 leakage happens through the casing-cement microannulus, cement-cement fractures, or cement-caprock interface. A casing-cement microannulus was simulated in [12] by using core-flood experiments conducted on a synthetic wellbore system. It was consisted of a cylindrical core cured with an embedded rectangular steel casing which had grooves to allow fluid flow. A mixture of supercritical CO_2 and brine flowed through limestone before entering the casing-cement grooves. Scanning electron microscopy (SEM) indicated that both the cement and casing were affected by CO_2-brine mixture.

Wellbore integrity problems can usually be divided into two main categories of; poor completion and abandonment, and the long-term stability of a wellbore in a CO_2-rich environment. Although CO_2 accelerates steel corrosion and converts Portland cement into mixtures of calcite and silica, the main aspect that needs to be considered is its impact on wellbore integrity as a function of the fluid dynamics, reaction kinetics, and stress state of the wellbore. The relative rates of chemical reactions and fluid flux

determine if the process is dominated by dissolution and continuous widening or whether the solid products of reactions precipitate on the interfaces which seals the interface against subsequent fluid flow.

The experiment design in [12] consisted of a 10-cm length of limestone to simulate the movement of CO_2 through reservoir or cap-rock prior flooding into a synthetic 6-cm wellbore constructed of Portland cement with an embedded rectangular steel casing. Since a confining pressure may probably seal the cement-steel interface, seven 0.2-0.8 mm deep grooves were carved on the steel surface and approximately 0.1 mm in the cement. It was ensured that fluid flow only just occurred through the cement-steel interface due to the extremely low permeability of the Portland cement. The results illustrated the formation of a 'wormhole' at the inlet of the composite limestone-cement/casing, while on the other end of the limestone core there was no trace of the 'wormhole' which was explained by the solution reaching an equilibrium within the limestone. There were signs of corrosion in both of the outlet and inlet of the cement. The initial permeability of the assemblage was around 0.52 Darcy (D), and following the experiment the system was flushed with brine and the permeability at residual CO_2 was re-measured to be approximately 0.67 D.

After the experiment, four sections were extracted from the cement-casing core. Examination of the sample by SEM indicated abundant evidence of chemical reactions between the CO_2-saturated brine, steel, and cement. The Portland cement did not show any notable erosion and CO_2 did not diffuse into it. The analyses disclosed the variation of the chemistry of channel deposits from approximately pure Fe- to approximately pure Ca- carbonates. Produced fluids from the experiment had abundant brown precipitates that were considered to be Fe-rich minerals obtained from the steel casing dissolution.

The carbonation included an extension of an orange colour, replacement of primary cement hydrate phases by calcium carbonates and the loss of residual cement clinker phases. However, the development of carbonation is a function of a diffusion process within clear carbonated and unaltered cement.

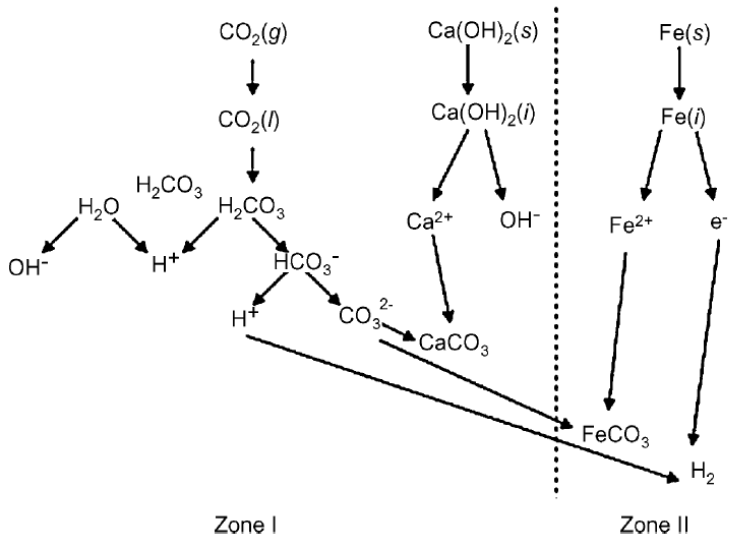

Fig. 2: Chemical reactions in the cement carbonation (Zone 1) and corrosion of the steel (Zone 2) and exhibition of the cement–casing contact in the wellbore [12].

A general combination of the work which was conducted by Carey et al. [12] and the works in [4,55,77] indicated that Portland cement is resistant to a mass loss in CO_2-brine systems. Carey et al. [12] noted that the diffusion of CO_2 into the cement was assumed to be a one-dimensional problem resulted in an effective diffusion coefficient ranging from 1.1×10^{-10} to 4.4×10^{-12} cm^2/s for depths of 50-250 μm. It seems that CO_2-brine fluids more corrode the standard steel casing rather than cement.

The acidic brine will affect the steel casing more than the cement. These studies confirmed the presence of iron carbonates in the gap between the steel casing and the cement. It shows a preferred corrosion of the steel casing exposed to the acidic brine (CO_2-saturated brine) rather than diffusion into the cement.

Fig. *2* simply illustrates reactions at the casing-cement interface resulting in formation of two main products of calcium carbonate and iron carbonates. The corrosion generally results in self-healing behaviour of the gap between the cement and the steel casing at the outlet position. The formation of a protective iron carbonate scale prevents further corrosion of the casing while the carbonated cement further protects the casing against considerable corrosion. Typically, corrosion rates decline with time due to the formation of scale on the surface of the casing. It was shown that scale formation decreases the corrosion rates of steel by two orders of magnitude compared to fresh steel [26]. Generally, the self-healing behaviour of a wellbore system is still uncertain and needs a systematic investigation of cement alteration exposed to CO_2-rich fluids [23].

The corrosion rates of mild steel in contact with high-CO_2 fluids was modelled by Han et al. [78]. A corrosion rate of 1.24 mm/year (at temperature: 0 ℃, partial pressure of CO_2: 1 bar, in brine of 1 wt% NaCl) to a maximum of 98.37 mm/year (at temperature: 100 ℃, partial pressure of CO_2: 1000 bars, in brine of 1 wt% NaCl) was predicted. Increasing salinity considerably reduces the corrosion rate; for example, a threefold increase in salinity 5 to 20% reduces the corrosion rate to around half of its initial value. The investigation of bicarbonate (HCO_3^-) impact on carbon steel exhibited that increasing salinity, in pH ranges of 4-7, declines corrosion rate [79]. Whilst at a higher pH (7-8), bicarbonate concentration increases due to a higher salt concentration which leads to a higher corrosion rate.

4.1 Conducted experiment on effect of gaps between the casing and cement on the rate of cement alteration

Table *3* summarises details of experiments which have been conducted to investigate effect of flowing CO_2-bearing fluids through gaps between casing and cement on their integrity.

Paper	Curing conditions	Method of experiment	Applied temperature condition	Applied pressure condition	Core dimension	Properties of fluid	Fluid rate/ pressure gradient	Aperture	Time-length of experiment	comment
[11]	• Class G cement • Curing time of Rod-cement sample:14 days	Flow-through	• Temperature for rod-cement sample: 60 ℃ • Temperature for cement cores: 65 ℃	• For rod-cement sample Confining pressure: 24100 kPa Pore pressure: 13780 kPa • For cement cores Confining pressure: 28940 kPa Pore pressure: 15160 kPa	• Diameter of 3.8 cm and length of 3 cm for cores which their permeability were measured • For Rod-cement sample: Inside diameter: 3.8 cm Outside diameter: 7 cm length: 9.55 cm	Brine salinity: 15,000, 60,000 and 80,000 mg/l of NaCl	N/A	• Aperture of cracks in cement: 3-5 μm • Aperture between casing and cement: 10-15 μm	90 days for cement cores	• Ethane was used instead of CO_2 to examine the impact of the annular gap and crack on the effective permeability of cement-casing assemblage • Presence of Both of gap between cement and casing and radial crack were investigated

[12]	• Class G cement • The steel was embedded in the centre of the cement core • Curing time: 1 month • Cement moulds were submerged in the $Ca(OH)_2$-saturated water	Flow-through	40 °C	• Confining pressure: 28 MPa • Pore pressure: 14 MPa	• Diameter: 5 cm • Length of steel-cement assemblage: 6 cm • Length of limestone core before the steel-cement assemblage: 10 cm	Brine composition: 25000 ppm NaCl, 4000 $CaCl_2$, 1000 ppm $MgCl_2$, and 200 ppm $MnCl_2$	Total volume of 50:50 co-injected CO_2 and brine: 6.2 litres	Depth of grooves in the steel: 0.2-0.8 mm and in cement: ~0.1 mm	394 hrs	Carbonation depth: 50-250 µm and depth of corroded steel: 25-30 µm after 394 hrs

Table 3: Experimental setup used by different authors for investigating the effect of gaps between cement and casing on CO_2 leakage

5 Investigation of leakage through the gap between cement and rock

Injected CO_2 steadily migrates upwards, due to the buoyancy force, until reaches caprock. This gas may be trapped just beneath of the caprock or continue its movement parallel to a tilted caprock [80,81]. Therefore, poorly cemented wells which penetrate the caprock are highly vulnerable to CO_2 leakage from the node of formation-caprock-cement as the leakage starting point. The low-quality bonding between the storage formation and cement provides a leakage pathway, albeit the permeability of this pathway should be higher than surrounding storage formation. Although it is sometimes violated because CO_2-bearing fluids move straight towards the node by reason of buoyancy forces and the storage structure geometry. Many studies are devoted to investigating the effect of CO_2 leakage on the aperture between caprock and cement, please refer to [10,12,29,47,51,59,69,71,82,83] to see more details.

5.1 Predominating phenomena

None of the Elovich and simple diffusive models were able to illustrate the observed silicon and calcium reaction concentrations (In the work of Walsh et al. [71]). Experiments actually exhibited a superdiffusive behaviour for the reaction-zone growth, and to address this problem it was suggested that expanding the reaction-front surface area could be incorporated into the modelling approach. Diffusive transport into the cement and advective transport along the cement-formation interface can be applied to investigate wellbore integrity. For example, at the Krechba carbon storage site, Algeria, a reactive transport model was applied by McNab and Carroll [84]. This model that benefited from a dual porosity modelling method postulating a Fickian diffusion for transport into and out of cement and an advective solute transport through the formation. The geochemical model developed by Walsh et al. [71] to compare the chemical changes of the cement neglects the impact of fracture geometry and dissolution of carbonate minerals on reactions. Even though this model may sound simple, it includes the precise regenerated development of reaction-zones and effluent chemistry in large-scale and long-term simulations. In this modelling, precipitation and dissolution were confined to the reaction fronts to reduce the computational cost of the simulation at larger scales and time intervals. The experimental results confirmed the transformation of the C-S-H to an amorphous zeolite phase, and examinations showed the most probable state for this transformation is analcime.

Duguid et al. [85] conducted an experiment in which cement cores were embedded in sandstone and limestone cylinders which are two most likely types of reservoir rock. It was exhibited that the cements embedded in the sandstone seem to be more vulnerable to degradation than those cement cores surrounded by the limestone rocks. Carbonation of different phases already present in the pores of the cement does not occur at the same time and, typically, calcium hydroxide reacts prior to C-S-H. At the beginning of the reactions $CaCO_3$ is stable due to the alkali environment of the pore. However, after a while, and by depleting $Ca(OH)_2$ and alkali phases from the pores, the pH reduces and leads to the

subsequent dissipating of the calcium in the major cement phases, therefore only a porous silica gel will remain. EQ3/6 (a software package for geochemical modelling of aqueous systems) of Wolery and Jarek [86] was applied by Duguid et al. [85] for modelling batch systems by considering limestone as $CaCO_3$ and sandstone as SiO_2. Results showed that the cement-limestone did not demonstrate a considerable alteration after being exposed to carbonated brine. Whereas the cement-sandstone samples experienced a clear change started from the interface of the cement and sandstone towards interior parts of the cement. The cement-sandstone composite experiments demonstrated a diffusion-controlled attack at both room temperature and 50℃ during the first 6 months of the experiment. Because the depth of penetration of the visible reaction zone showed a linear growth versus Boltzmann variable, $t^{1/2}/r$. Where r is the shortest distance between measurement point and the edge of the sample, and t is time,. During the next six months, the slope of penetration depth into the cement in contact with the sandstone versus Boltzmann variable or the square root of time altered, probably due to a change in the governing dissolution reaction and pores becoming clogged by $CaCO_3$ precipitation when exposed to carbonated brine at a pH between 3 and 5.

5.2 Change in cement properties

Recently, Connell et al. [87] conducted two core flooding experiments at similar conditions to geological carbon sequestration using a composite of cement-sandstone core plugs in order to investigate cement degradation at the cement-formation interface. Given that the permeability of intact cement is exceedingly low and that typically the measurement of degradation is time-consuming, in order to solve this problem a composite of cement-sandstone core plug was constructed which allowed enough flow of water on the basis of the high permeability of the sandstone. Cement and sandstone halves were stacked together in the experiment, therefore in practice no aperture existed between them. Brine was prepared by mixing known quantities of NaCl, $MgSO_4$, and $CaCO_3$ with water. Cement degradation requires two conditions to be met; firstly the undersaturated formation waters in calcium and carbonate ions, and secondly a flow of fresh water into the cement-sandstone interface to transport these solutes away. Non-carbonate reservoirs are more prone to cement degradation due to undersaturated formation waters in calcium and carbonate. Despite the expected increase in porosity of the amorphous and depleted layers, permeability exhibits a decline probably due to the formation of calcium carbonate, the low density of the amorphous silicate, and enhanced compressibility of changed layers. In addition to the reactions that affect cement and the transport behaviour during its exposure to CO_2, its mechanical properties also undergo an alteration which impacts on the porosity and permeability of the cement. A model was represented by Walsh et al. [10] based on the nano-indentation, x-ray tomography, and digital image correlation data. This model characterises the relevance of the reaction layers to the mechanical response of the cement interfaces. The model was developed to relate the fracture conductivity to the applied stress and the extent of reaction. In this experiment, it was assumed that the majority of flow occurred through the fracture rather than the cement matrix, therefore, the hydraulic aperture was used to represent the hydraulic properties of the cement-rock core. The linear relationship between effective stress and the hydraulic aperture was based on the fact that every model exhibits a linear behaviour over some ranges. However, changes in the matrix permeability were omitted from calculations and the fracture was considered as the main flow path. The hydraulic aperture decreased because chemical reactions weaken the asperities (asperities keep the fracture aperture open) in the cement-rock interface. This process leads to the fracture closing due to confining pressure burden on the sample. Nano-indentation measurements showed that the amorphous layer is the most compressible layer, followed by the calcium-depleted layer, while calcium carbonate layer remains the stiffest layer, equal or just above the strength of the unreacted layer against deformation. A reaction model was developed by Mason et al. [9] in which the reaction path is linked to the mechanical response of the changed zones and their corresponding impact on the wellbore performance in CO_2 storage environments The majority of the amorphous component was assigned to the amorphous aluminosilicate with similar composition to the zeolite minerals of the mordenite or clinoptilolite. This work illustrated that during the exposure of cement to CO_2, an alteration of C-S-H occurs simultaneously with calcium carbonate precipitation, resulting in a final phase of amorphous zeolite rather than amorphous silica.

The depth of penetration of the reaction front into the cement, in work of Walsh et al. [29], was about 2 mm after eight days. This value was greater than depths reported in [12,25,55]. This observation was

attributed to the differences in brine chemistry and flow rate. Generally, experiments conducted under flow-through conditions show deeper penetration rather than the static condition, whereas by decreasing the flow rate the thickness of the calcium carbonate zone increases. Depending on brine chemistry and at larger time scales, the precipitation of calcium carbonate and the volume fraction of calcite determine the relative speed of leading edge of the calcium carbonate layer and depleted region. Tortuosity also influences the general rate of propagation. Simulations illustrated an increase in the porosity value, while total permeability decreases, in part as a result of swelling in the amorphous silicate layers, and mechanical degradation of the asperities acting as pillars. Numerical modelling of the carbonation process by Geloni et al. [51] which includes portlandite dissolution and precipitation of calcium carbonate simultaneously by partially C-S-H dissolution showed, in contrast, a reduction in the porosity. During the next phase, however, the so-called degradation process mostly was dominated by dissolution of precipitated calcium carbonate, results in a porosity increase. The simulation predicted that the reaction front penetrates 0.12 m into cement during a period of 100 years.

5.3 Conducted experiments on the effect of the gaps between cement and rock on CO_2 leakage

Table *4* shows information of experiments which have been conducted to investigate the mutual impacts of flow of CO_2-bearing fluids on gaps between cement and rock, and vice versa.

Paper	Curing conditions	Method of experiment	Applied temperature condition	Applied pressure condition	Core dimension	Properties of fluid	Fluid rate/ pressure gradient	Aperture	Time-length of experiment	comment
[29]	• Class G Portland cement • Curing in accordance with ASTM Test Method C114	Flow-through	60 ℃	• Confining pressure: 24.8 MPa • Outlet pore pressure: 12.4 MPa	• Diameter: 15 mm • Length: 30-37 mm	Brine salinity (mol/L): NaCl:1.01 Na_2SO_4: 3.69*10^{-2} $MgCl_2$:1.59*10^{-2} $CaCl_2$: 3.53*10^{-2} $NaHCO_3$:7.92*10^{-3}	Constant flow rate: 1 cc/min	20-100 μm deep pockets using bead-blasting method on the surface of the cement half	8 days	• The caprock halves consist of full dense calcite-cemented, quartz-sandstones. • Depth of reaction front penetration: 2 mm.
[9]	• Class G Portland cement • W/C: 0.4 • Initial setup time;1-2 days • After being placed in the autoclave: Temperature: 50 ℃ Pressure: 15 MPa • Curing time-length in 1 %wt NaCl: more than 28 days	Flow-through	60 ℃	• Confining pressure: 24.8 MPa • Pore pressure: 12.4 MPa •For additional NMR experiment, pore pressure: 6.5-7.0 MPa	• Diameter: 15 mm • Length: 37 mm	• Initial chemistry of brine and dissolved CO_2 are representatives of CO_2-EOR • Composition (mol/kg H_2O): NaCl: 1.01 Na_2SO_4: 0.0369 $MgCl_2$: 0.0159 $CaCl_2$: 0.0353 $NaHCO_3$: 0.00792	• Average flow rate: 0.5 cm^3/min • For additional NMR experiment, flow rate: 0.10 cm3/min	Aperture: 15 μm	The core was equilibrated with brine for 7 days prior to reaction with CO_2-saturated brine for 7 days	• The caprock halves consist of full dense calcite-cemented, quartz-sandstones • CO_2 saturation at pCO_2= 3MPa with brine for 8 hrs • The Final result of C-S-H alteration was an amorphous zeolite rather than an amorphous silica and this change was assumed to occur simultaneously with the calcium carbonate precipitation. • Thickness of different layers: amorphous silica layer: 930 µm carbonate layer: 190 µm depleted region: 650 µm

[71]	• Class G Portland cement Preparation according to ASTM Test Method C114	Flow-through	60 ℃	• Confining pressure: 24.8 MPa • Pore pressure: 12.4 MPa	• Diameter: 15 mm • Length: 30-37 mm	Brine was initially in equilibrium with calcite and dolomite at 60℃.	• Constant flow rate: 0.01, 0.025, 0.05, and 0.1 mL/min • 12 hrs takes for solving of CO_2 (pCO_2: 1-3 MPa) in brine	Aperture varies between 21.9 μm to 143.7 μm	4, and 8 days	• The caprock half is a full dense calcite-cemented, quartz-sandstone • Three main types of surface were supposed at the interface of cement and caprock including surface with channel, gridded surface, and rough surface. • 13 core-flood experiments were conducted. • Boundary between the unreacted cement and portlandite depleted regions moved around 2 mm in 8 days.
[85]	• Class H cement • W/C: 0.38 • Curing time-length: 7 months • Cement samples were submerged in 0.5 M NaCl	Batch system	Room temperature and 50℃	Atmospheric pressure	The cores were built by cutting off stone cores (with diameter of 55 mm and ~ 10 cm in length which have a 25-mm diameter hole drilled off centre filled with cement) into nearly 1-cm-tall slices	• pH of introduced brine into sandstone-cement core: 3-5 • pH of introduced brine into limestone-cement core: 5-7	N/A	N/A	Samples were removed from the reactor at 1, 2, 3, 6, and 12 months from the beginning of the experiment	• Depth of reaction front penetration into sandstone–cement cores: 270-322 µm over a period of 1 year at the nearest position to the brine-stone interface and room temperature; up to 577 µm over a period of 1 year at the same position and 50 ◦C. • Experiments at 50 ◦C limestone–cement and room temperature limestone–cement never showed any visible reaction zone within the cement.
[87]	• Class G cement	Flow-through	50 ℃	Confining pressure: 10 MPa	• Diameter: 53 mm • Length: 25 mm	• Brine salinity in experiment 1 (in g/l) NaCl: 20.7 $MgSO_4$: 2.6 $CaCO_3$: 0.78 • Brine salinity in experiment 2 (in g/l) NaCl: 1 $MgSO_4$: 0.3 $CaCO_3$: 0.5	The upstream works at constant flow rate while at the downstream position fixed pressure dominates on flow	The cement was casted around a sandstone block and cored on perimeter which cement-sandstone interface bisect the core, therefore actually there is no initial aperture	104, and 105 days	The core sample is a composite of cement and sandstone halves

Table 4: Experimental setup used by different authors for investigating effect of gaps between caprock and cement on CO_2 leakage

6 Geomechanical investigation

The cement slurry design is of great importance because the higher flexibility of this system results in being able to sustain a large pressure differential across the cement plug [88]. In fact, expansion due to internal casing pressure or temperature, cyclic pressure fluctuation, thermal gradients, and long-term cement shrinkage may lead to cement sheath failure providing pathways for leakage of CO_2 upwards [89,90].

6.1 Change in mechanical properties

A fractured cement similar to the conductive pathways within a cemented annulus was examined by Huerta et al. [72]. Hydraulic conductivity was measured under confining stress to investigate the effect of the increasing confining pressure on the size of the aperture. The probable self-sealing behaviour of the conductive pathways under the constant effective stress was confirmed. Although there may also be

other pathways for the leakage of CO_2 to the surface, such as microfractures, microannulus, or channels as the most potential conduits. Lack of good quality bonding between the cement and casing or surrounding rock results in microannulus. Microfractures are formed by tensile stress of cement. The incomplete replacement of mud by slurry or the permeation of gas into the cement before setting can lead to the formation of channels, which are the most prevalent leakage conduits. Huerta et al. [72] speculated the assumption of plastic behaviour and deformation of the cement under stress to block the leakage path. To accelerate the process of degradation in their experiment HCl was used, even though the reaction of cement with HCl and acidified brine is completely different although the effect on the mechanical strength is the same [25,91]. For the same change in the confining pressure, the moderate reaction of fracture with a low pH brine resulted in an aperture alteration twice as much as in the unreacted fracture. This may be caused by the loss of mechanical strength on the fracture surface due to the degradation. Nevertheless, the developed reaction of the fracture with low pH brine leads to a significant plastic deformation and lowering of the confining pressure to its initial value.

The occupied space of the portlandite after dissolution becomes a part of the connected macroporosity, while calcium leaching of the C-S-H leads to no evident change in the nanoporosity nor in the mechanical continuity of the microscopic solid phase [92]. Two main asymptotic states of equilibrium are expected, firstly an unchanged cementitious material, and the other is the state in which calcium concentration is homogeneously leached from the cementitious material and no further change is expected to happen in the calcium concentration of the solid phase. Therefore, the spontaneous alteration of leaching can be predicted by following non-equilibrium thermodynamics between these two asymptotic states [92]. The built-in framework predicts that the elasticity domain of cementitious materials is influenced by chemical degradation and mechanical loading. The impact of mechanical changes on the portlandite dissolution kinetics, however, were assumed negligible. C-S-H dissolution does not change the texture but composition which is considered as a second dissolution front that propagates behind the portlandite dissolution front. Indeed, portlandite dissolution affects the present pore space and provides an additional pore space for solid phase expansion in the period of plastic dilatation in compression which postpones the failure along the shear planes, whereas dissolution of the C-S-H results in a net chemomechanical softening [93].

Measurement of static moduli and the mechanical strength by a triaxial apparatus, and dynamic elastic moduli by S and P waves demonstrated carbonation as a reason for porosity decrease, permeability change, and an increase in mechanical properties including mechanical strength and elastic moduli [75]. Dried samples exposed to wet supercritical CO_2 illustrate a homogeneous carbonation without an evident carbonation front, indicating that wet supercritical CO_2 diffuses into the dried unsaturated cement core rapidly. Wet specimens showed an annular carbonation with a sharp carbonation front (11-mm movement towards internal parts of the cement in the period of 62 days). The samples with annular carbonation were highly sensitive to confining pressures up to 15 MPa, which can be interpreted as the elastic closure of micro-cracks. Annular carbonated cement samples suffered more damage than homogeneous carbonated samples as a probable result of difference in stiffness between the carbonated and dissolution zones or pore overpressure due to precipitation. Samples with a carbonation front exhibited a high degree of sensitivity to pressure, which can only be explained by the extension of the microcracks around the carbonation front leading to the degradation of the mechanical strength and an increase in permeability when deviatoric stress is present. It is notable that considering static conditions for carbonation may result in degradation of cement but not as severe as when the core cement is flooded with CO_2-rich fluids.

Due to the inhomogeneous carbonation in samples, conventional mechanical tests are not universal and representative of changes. Accordingly, the scratch examination of the sample at the length scale of millimetres and nano-indentation at the length scale of micrometres were performed to evaluate the changes of the mechanical properties due to chemical reactions. Lecampion et al. [94] examined the macroscopic alteration of the material failure properties in a closed system at high temperature and pressure between carbonated and unreacted zones. They used macroscopic scratch and nano-indentation grid which probes material changes at smaller scales. For any value of the fugacity of CO_2, the Gibbs free energy of the portlandite and C-S-H reactions with CO_2 is negative and these reactions derive forward to be completely depleted from the reactants. Scratch tests provide this opportunity to measure

the mechanical strength of the specimens at macroscopic scales without any enormous damage to the sample. It should also be noted that the scratch test is widely being used for the sedimentary rock characterisation. This investigation clearly illustrated two main zones: a stronger area which matches the carbonated rim and the zone in the centre of the core with an average horizontal cutting force similar to the unreacted cement. In general, the pure cutting force is imposed on the cutter which is used by the scratch test. The obtained thicknesses for the carbonated zones (thickness of carbonation rim was 2-3 mm after 88 hrs in samples exposed to wet supercritical CO_2 or CO_2-saturated water and 5-7 mm after 523 hrs) from the scratch test were of the same magnitude which were visually measured. It was also reported that carbonation increases the strength of cement. Two main results were obtained from the chemical analysis. Firstly, the carbonated matrix was initially composed of the silica gel, calcite, and declassified C-S-H. Secondly, representative elementary volume (REV) scale increased which means more heterogeneities at small scale. Both of the scratch and nano-indentation tests supported the existence of a centre with properties very similar to the unreacted cement and a carbonated zone which is stiffer than initial cement. Studies at lower scales indicated that C-S-H matrix incurred a notable change [94].

6.2 Response of leakage pathways affected by mechanical degradation

The carbonation process in cement leads to the formation of cracks and a remarkable strength loss resulting in a large difference between the calcite layer and unaltered cement of the sample in terms of mechanical strength. For example, the carbonation process results in difference between Young's moduli of unreacted cement and calcite layer which leads to the calcite layer compression [45]. Measurements of the hardness and Young's moduli values at reaction zones locations indicated a high degree of heterogeneity at scales of micrometres [9].

Cyclic loading of cement cores illustrated a decline in aperture size with increased confining pressure, work hardening, and hysteresis in loading and unloading cycle [73]. It was shown that mechanical weakening of the cement core due to reaction eventuates in a fast closure of aperture with increasing confining pressure. In fact, a combination of the degradation of the cement and decreasing fluid pressure could result in self-healing behaviour of leaky wellbore cements. The fracture clogging may also result from a reduction in the strenght of the asperities which keep fractures open or swelling in the amorphous silica layer immediate to the fracture. However, Brunet et al. [8] suggested that the dissolution of cement and high flow velocities may mechanically remove material within fractures which increases the probability of precipitation and blockage. Mechanical displacement of cement grains elevates the chance of aperture size reduction due to the trapping these grains in the fracture.

Self-healing behaviour of the cement in reaction with CO_2-rich fluids is highly likely either due to mechanical softening of reaction products, precipitation, and volume changes of reaction products. From a thermodynamical view, the reaction of the CO_2-water system with Portland cement is rapid, however, Portland is able to isolate wells from surrounding formation and maintains that state due to the coupled flow of reactants and the rate of reactions. In fact, the cement carbonation leads to reduced permeability and enhanced mechanical strength [23].

7 Discussion

7.1 Hydration and curing

The cement Portland clinker is generally formed of tricalcium silicate ($3CaO.SiO_2$ or C_3S), dicalcium silicate ($2CaO.SiO_2$ or C_2S), tricalcium aluminate ($3CaO.Al_2O_3$ or C_3A), and tetracalcium aluminoferrite ($4CaO.\ Al_2O_3.Fe_2O_3$ or C_4AF) which are accounted for solid phase solution [95,96]. The addition of water to the cement Portland is an exothermic process. C_3A hydrates faster than the other cement components and causes early strength developing, however, setting time is controlled by adding gypsum. C_3A is highly soluble in water, even more than C_3S, and releases large amount of energy which may result in cement setting within a few minutes. This phenomenon known as flash set controlled by adding gypsum [96]. C_4AF has little effect on physical properties of the cement paste and its hydration reaction are similar to those of C_3A [83,95,96]. The reaction of C_3A in presence of gypsum with water results in formation of ettringite ($Ca_6Al_2O_6(SO_4)_3.32H_2O$). Usually, the gypsum content of cement is depleted prior

to the complete consumption of C3A. The produced ettringite reacts with C_3A and water to forms monosulfoaluminate ($3Ca_4Al_2O_6(SO_4).12H_2O$) [96]. In fact, most of ettringite converted to monosulfoaluminate within the first days due to lack of gypsum as follow:

$$Ca_6Al_2O_6(SO_4)_3.32H_2O + 2C_3A + 4H_2O \rightarrow 3Ca_4Al_2O_6(SO_4).12H_2O \quad \text{Eq. 8}$$

C_3S reacts faster than C_2S and is responsible for strength at all the times while C_2S mostly affects the final strength development of the cement paste [95]. The reactions of C_2S and C_3S with water produce C-S-H and portlandite:

$$2C_3S + 6H_2O \rightarrow Ca_3Si_2O_7.3H_2O + 3Ca(OH)_2 \quad \text{Eq. 9}$$

$$2C_2S + 4H_2O \rightarrow Ca_3Si_2O_7.3H_2O + Ca(OH)_2 \quad \text{Eq. 10}$$

C-S-H (here $Ca_3Si_2O_7{\cdot}3H_2O$) is the primary binding phase which is amorphous with Ca:Si ratio ranging from 1.5 to 2.0. Portlandite is a crystalline phase which occurs in hexagonal plates. Generally, C-S-H composes up to 70% of hydrated cements, and between 15 to 20% of the hydrated cements are formed of portlandite [30,96].
The oilwell cementing is usually accompanied by adding different types of additives to modify the rheological properties of cement slurry to bear underground formation conditions and at the same time remain pumpable during the cementing operation. The high pressure and temperature affects the hydration process. The hydration process is complicated, since C-S-H is a non-stoichiometry product, and combining new additives into the cement slurry make the prediction of the cement set composition more difficult [97]. The National Institute of Standards and Technology (NIST) provided free models to simulate cement hydration and degradation [98]. Moreover, some attempts have been done to calcify the resultant composition of cement after hydration [97,99–101]. Nonetheless, it is still challenging to know the final composition of cement after the hydration under high pressure and temperature conditions.

7.2 Preparing method of cement cores

The experimental method for examining the impact of the aperture between the casing and cement on CO_2 leakage, typically based on embedding a steel casing within cement [11,12]. Moreover, coupled half cylindrical cores were designed for evaluation of the separation effect between rock and cement on the CO_2 leakage process. Generally, prior coupling, the cement half core is subjected to sandblasting for generating an aperture of an arbitrary size to prevent it from closing due to confining pressure [29,66].

Investigations into the alteration of cement due to CO_2-bearing fluids' exposure at the interface between cement and storage formation or cement and caprock have been conducted by using cylindrical cores composed of cement and rock halves. Generally, the gap between them was maintained by applying asperities or cement surface sandblasted heterogeneously/regularly using special masks for obtaining an arbitrary separation. Sandblasting may also be applied to achieve regular patterns or separation gap for evaluating cement alteration rate in presence of cracks. Likewise, a Brazilian method commonly used to develop heterogeneous cracks through cement cores. To investigate cement alteration surrounded by different rock types, Duguid et al. [85] drilled a stone rock off-centre and filled in the hole with the slurry to set. This system probes the impact of flow/diffusion through a rock prior to encountering cement sheath. Numerous studies simulated the real variation that occurred in brine composition when passing it through a formation surrounding a well before reaching the cement interface by altering brine composition to be saturated with minerals present in the formation (e.g., works in [9,29]). On the other hand, carbonate or sandstone beds were embedded before core samples in some studies to simulate the actual underground formation which brines pass through [12].

7.3 Brine salinity changes prior to cement exposure

CO_2-bearing fluids prior to being exposed to cement, in forms of well lining and cappings, pass through rocks such as limestone, dolomite, or sandstone as the most probable occurring rock types in storage sites. This process alters the salinity of the CO_2-bearing fluids, increasing the calcium concentration as a result of an interaction with carbonate rocks surrounding the cement. This interaction reduces their capability in dissolving more calcium from the cement. On the other hand cements surrounded with

clastic sedimentary rock are more vulnerable to damage due to exposure to the CO_2-bearing fluids. To simulate this condition, typically, researchers try to change brine salinity to match the brine composition and its acidity under sequestration conditions when encountering the cement surface. Building cement-rock assemblies is another way which mimics the passage of CO_2-saturated brine through rocks prior reaching the cement surface in underground formations [12,27,85]. Although, reactions between aqueous phases are fast enough to be considered in their equilibrium state, reactions between solid and aqueous phases are not fast and should be kinetically investigated. In underground formations, due to low velocity of brine close to the abandoned wells, CO_2-bearing fluids have sufficient time to reach an overall equilibrium during passing through rocks surrounding the well cements. Therefore, short-length rocks may not give required time for passing fluids to equilibrate with the solid phases. This should be considered in experimental design.

A simple solution is to add components to CO_2-bearing fluids which are similar to the fluid composition expected to obtain from long-term contact between CO_2-bearing fluids and rocks under geo-sequestration conditions [9,29,64,87]. This method seems to be safe which increases confidence in the results and saves more time.

7.4 Role of general geo-sequestration conditions

A higher amount of CO_2 dissolves in brine with increasing pressure, while increasing the temperature and salinity reduces the CO_2 solubility in brine [37,38,102]. A high ratio of portlandite to porosity results in the forming of sharp calcium carbonate precipitation zone which makes diffusion of CO_2 into cement more difficult. In contrast, the low-portlandite and high-porosity ratio leads to a reduction in the probability of clogging [57]. The applied ratios of water to cement for building the slurry have a highly determinative impact on the strength and durability of the cement. The lower the water to cement ratio, the higher the durability and strength of the cement [23,83,103]. Furthermore, curing of cement at pressure and temperature associated with underground formation commonly increases the resistance of cement against carbonic acid attack [25]. Additives also change the rate of the front penetration into the cement, such as pozzolan-amended cements which are harder than neat cement types but the rate of penetration is noticeably higher than for neat cements [44,58,61]. Under geo-sequestration conditions, exposing cement to CO_2-bearing fluids at static or flow-through conditions affects the boundaries of cement and CO_2-bearing fluids to a great extent. Under static conditions, after a period of time the reactions between the solid and aqueous phases reach an equilibrium which may restrict the depth of penetration, depending on the compositions of both. In spite of the static condition, subjecting a cement type to the flow of CO_2-bearing fluids continuously brings fresh CO_2-bearing fluids in contact with the cement, thus the penetration front would probably continue to its motion within cement under this condition.

7.5 Formed zones and fronts

Generally, cement exposure to CO_2-bearing fluids results in the formation of four main zones including an unaltered cement zone, a portlandite dissolution zone, a calcium carbonate precipitation zone, and an amorphous silica gel zone [4,18,25,35,50,47,58,73,85,104,105]. This includes three corresponding fronts as follows: a portlandite dissolution front, a calcium carbonate precipitation front, and a calcium carbonate re-dissolution front dominate the formation of the four main zones [18,62,92].

Calcium leaching from C-S-H occurs in both the calcium carbonate precipitation zone and the amorphous silica gel zone [33]. Calcium carbonate is more stable than portlandite in contact with the CO_2-bearing fluids. The process of CO_2 dissolution into pore water and the conversion of portlandite to calcium carbonate (or calcite which is the most stable form of calcium carbonate) is referred to as carbonation. Most of the so-called degradation processes occur at the calcium carbonate re-dissolution front or amorphous silica gel zone which is sometimes referred to as the bicarbonation process [83]. Generally, the main cement alteration process happens during the first hours or days of tests [11,18,25,27,29]. This phenomenon confirms that a decrease in porosity and permeability in the calcium carbonate precipitation zone prevents CO_2-bearing fluids moving further into the unaltered cement zones, although porosity increases due to portlandite dissolution and bicarbonation. Carbonation processes typically start at a higher pH in comparison with the required pH for activating bicarbonation processes [33,85]. The

movement of the carbonation front into cements and its thickness is a function of the pressure, temperature, salinity of ubiquitous brine, mineralogy of the cement, and boundary conditions.

7.6 Predominating phenomena

Reaction kinetics are typically faster than diffusion rate, therefore diffusion was assumed to dominate the permeation of fluids into cements. Besides, advection may also be considered responsible for the transport along the interface of cement and rock, cement and casing, or cracks in cements [13,26,85,106]. In theory, Fickian diffusion was postulated for transport into cement in many studies, even though in some experiments this rule is violated. Fast reaction of calcium carbonate probably justifies assumption of neglecting reaction kinetics. Although formation of metastable forms of calcium carbonates, i.e., vaterite and aragonite, emphasizes effect of carbonation kinetics. In fact, mineral-solution equilibrium is established slower than reactions occurring in aqueous phase. Therefore, involving reaction kinetics represent the reality of process more accurately.

Movement of CO_2-bearing fluids within cement or rock is accompanied by reactions between solid and aqueous phases and reactions between components present in aqueous phase together. Generally, reactions occurring within aqueous phase are faster than dissolution of solid phases in CO_2-bearing fluids. Although, it is not an accurate assumption but still possible to assume reaction rates of solid phases with aqueous phases are also fast. This assumption simplifies the formulations dominating movement of CO_2-bearing fluids within cement by removing mass action laws (describing dissolution of solid phases in aqueous phase) from consideration. Due to high speed of reactions involved in this process in comparison with the diffusion of species, the dominating process will be the diffusion phenomenon. Depending on geo-sequestration conditions this assumption may be an acceptable simplification [15,24,26,43,49,47,51,57,64,69,85,106]. In some cases, reactions between the solid and aqueous phases are not fast enough to neglect their impacts. The reaction rates also affect the concentration of passing species through the porous medium. Thereby, it will be necessary to include their contribution to the process by considering mass action laws. The added sections makes the governing equations more difficult, since they are differential equations which should be solved along the algebraic equations (representing fast equilibrium states) in each time step simultaneously with diffusion equation. Albeit, this methodology increases the accuracy of predictions, but, it is time-consuming [25,31,33,43,45,57].

7.7 Impact of residence time

Typically, the length of time in which a cement surface exposed to CO_2-bearing fluids is called residence time. A long residence time means that fluids have enough time to become closer to the equilibrium state of reactions between the solid phase and the aqueous phase. As a result, the fluid phase is saturated by the leached calcium content from the degraded cement. Based on the difference in the concentration of calcium content between the fluid phase and the pore fluid, the diffusion phenomenon motivates depletion of calcium from the cement matrix into the fluid at the interface. The saturated CO_2-bearing fluids regarding calcium gradually moves along the crack or the gap. In the next positions along the interface, the highly calcium saturated fluid phase starts to precipitate due to more calcium content compared to the adjacent cement pores, and pH reduction. In the short-residence times, the entry fluid degrades the inlet areas of cracks or gaps but not deep as much as the long-residence times. The lower calcium content, the lower affected pH degree, and shorter contacting times at downstream areas reduce the risk of calcium precipitation in these areas. Therefore, a stronger acidic fluid increases probability of degradation, even in the case of probable calcium precipitation on the surface of cements [15]. It seems that the long-residence times lead to self-healing behaviour while the short residence-times may not affect the aperture size or even widen the separation under more severe conditions. It is reasonable to assume the self-healing behaviour as a default change that may undergo during the cement exposure to CO_2-bearing fluids. This is due to low-velocity which is mostly governing on the near abandoned well [8,48,58,66,107]. To separate the self-healing from the non-sealing behaviours, Brunet et al. [8] and Iyer et al. [107] developed maps based on the initial residence time and the initial fracture aperture which determine a threshold for self-healing behaviour.

Overall, residence time is highly determinative of the fracture behaviour, self-sealing and opening. A long residence time increases the pH and Ca^{2+} concentration in the fracture, and calcium carbonate

precipitation which eventually leads to flow reduction. This phenomenon results in a positive feedback that under constant pressure gradient accelerates the self-sealing process. During short residence times, brine is replenished quickly which reduces the pH and Ca^{2+} concentration in the fracture. Accordingly, the dissolution of cement matrix continues which keeps the fracture open or even widens the aperture. [8,48,58,66].

7.8 Changes in porosity and permeability

Porosity increases due to portlandite dissolution and calcium leaching from the silica gel layer right after the cement-brine interface. In this case, cement mechanical strength degrades. In the zone between silica gel layer and portlandite dissolution, typically calcium carbonate precipitation occurs. This phenomenon may increase the mechanical strength of this zone to or just above the unaltered zone, and leads to a porosity reduction [10,27,45,72,75,94,108,109]. Although the dissolution of calcium hydroxide may result in a slight increase in porosity [25], C-S-H dissolution contributes substantially to porosity increase [57].

Generally, the altered cement matrix shows a permeability variation from the cement-brine interface to the inner parts of the cement which no alteration occurred and mostly called the unaltered zone. The permeability of the unaltered zone remains intact. The dissolution of portlandite in the next region adjacent to the unaltered zone increases the permeability in this zone as a result of porosity improvement. Thereafter, calcium carbonate precipitation decreases the porosity which leads to decrease in the permeability and increase the mechanical strength [27]. Close by the cement-brine interface, the degradation of the C-S-H phase causes the permeability enhancement. Therefore, the overall matrix permeability depends on the relative direction of flow with respect to the diffusion. The permeability of the altered cement, when the directions of flow and diffusion are parallel, shows a reduction since the calcium carbonate precipitation zone acts as a barrier to the flow. The averaged permeability increases for the flow perpendicular to the diffusion direction. The reason is due to permeability increase in the amorphous silica gel zone and the portlandite dissolution zone [45]. The permeability of cement is also a function of the hydration process undergone by the cement. The higher the degree of hydration the lower the permeability [25].

Generally, cracks and gaps are more potential pathways for the CO_2 leakage rather than the cement matrix itself. The high permeability of the cement matrix increases the concentration of calcium leached from the cement to the crack. This process enhances the probability of clogging at the downstream positions. In contrast, high crack/cement matrix permeability leads to less dense calcium precipitation zones [8]. The behaviour of cracks or gaps being either self-healing or open is a strong function of the residence time, the aperture size, the confining pressure, and the chemical reactions occurring during the process. The carbonation process and multiphase flow can reduce the permeability [10,23,75]. The permeability also decreases as a result of the low flow rate within the cracks. In fact, the low flow rate increases time of CO_2-bearing fluids exposing to the cement surface [64,66]. The degradation of mechanical strength in pillars and asperities, which keep cracks open, and the confining pressure may reduce the aperture size. Moreover, the amorphous silica gel formation is accompanied by the swelling process which also decreases aperture size [29]. The reduction in the aperture size will result in the permeability reduction or the self-healing behaviour.

7.9 Modelling

Modelling the long-term behaviour of cement degradation is imperative. In fact, short-term experiments cannot be representative of cement durability compared to extremely long periods of hundreds or thousands of years such as the prediction of penetration depth after 30 years which were carried by Kutchko et al. [55]. Modelling behaviour of cement exposed to CO_2-bearing fluids simply provides a framework to determine its stability during length of time beyond experiment duration. Many experiments, however, indicated that most of the alteration occurs during the first hours or days of exposure [11,18,25,27,29]. Besides, conducting a sensitivity analysis regarding acidic environment conditions to find controlling variables increases the cost of experiments.

The CrunchFlow code developed by Steefel et al. [110] is applied by numerous studies (for example in [8,31,45,57,66,69]) which combines effects of diffusion, advection, and reaction to model mass conservation of chemical species transport which is given by:

$$\frac{\partial(\phi C_j)}{\partial t} = \nabla.(D\nabla C_j) - \nabla(qC_j) + R_j \quad (j = 1,2,3,\dots n) \qquad \text{Eq. 11}$$

where ϕ is porosity, the term on the left side of Eq. 11indicates change in the concentration Cj of the component j (mol/m3), the first, second, and third terms on the right side of Eq. 11 stands for chemical species transport due to diffusion, advection, and reaction respectively, D is the combined diffusion-dispersion coefficient (m^2/s), q is the Darcy velocity (m^3/m^2s), and R_j (mol/m^3s) is total reaction rate obtained from summing up rates of precipitation and dissolution of involved minerals. Modelling of the presence of a fracture in cement, a gap between cement and casing, or between the cement and surrounding formation generally is based on the assumption that cement permeability is extremely low, thereby fracture/gap is the dominant flow path [10,12,14].

8 Summary

This paper provides a review of the works which have been conducted to investigate changes in the cement matrix exposed to CO_2-rich environments. This review illustrates that significant development has been made during the last two decades in better understanding the interactions of the CO_2 and cement to prevent the leakage of CO_2 through the well cement. The following summarises the most outstanding aspects which have been reviewed:

- Studies investigating the cement matrix alone in CO_2-rich environments disclosed that typically four main zones are being developed during the course of the cement exposure to CO_2-bearing fluids. However, sometimes the fronts have been used to describe the separation of these zones and their movements within the cement. Typically, these experiments studied under static conditions, since authors believed that in the close vicinity of abandoned wells fluid velocity is very low which can be neglected.
- To examine mutual effects of cement cracks on the CO_2 leakage and vice versa, these experiments have been conducted under flow-through conditions. Depending on the residence times of flow through cracks within the cement and acidity degree of CO_2-bearing fluids, cement could degrade quickly. This can occur when CO_2-bearing fluids acidity degree is high and residence times are short. This results in cracks widening and more CO_2 leakage. Whereas, generally, the low degree of acidity and long-residence times provide enough time for precipitation of calcium content downstream that makes the flow paths narrower or even block them.
- Assemblies composed of the cement and steel casing, generally, showed that the steel casings are more vulnerable to be corroded even in the presence of cement. To examine the effect of CO_2-bearing fluids on the steel casing adjacent to cement, cement-casing samples were undergone flow-through experiments. Deeper corrosion on the surface of the steel casing and presence of the Fe- components at the effluent confirm more inclination of the flow to affect the surface of the casing rather than cement. However, in some cases production of scales on the surface of the casing may prevent further corrosion or may even clog the leaking CO_2-bearing fluids downstream.
- Studies exploring the quality of the bonding between cement and surrounding rocks, typically, confirm that the cement matrix have been more damaged due to exposure to CO_2-bearing fluids. In fact, fluids composition alters prior reaching the well cement. Limestone rocks surrounding the well cement increases the degree of the calcium concentration of CO_2-bearing fluids before encountering the cement. This process reduces the capability of the cement to dissolve more calcium content from the cement. In contrast, the composition of fluids passing through the sandstone rocks surrounding the well cement remains constant regarding the calcium concentration, therefore they will have this ability to leach more calcium from the well cement. It should be noted that residence time is highly determinative of the rate of cement degradation.

- During cement exposure to CO_2-bearing fluids, the geomechanical properties of the affected areas also change. Except for the $CaCO_3$ precipitation zone which shows a low increase in mechanical strength, other affected areas decline in that term. The relationship between the geomechanical changes and their impact is complicated. Despite the common expectations, the degradation of cracks surfaces causes pillars and asperities lose their integrity, thus the crack walls become closer to each other due to confining pressure and may even results in clogging. Given the increasing compressibility due to the calcium leaching from the affected areas, except for calcium precipitation zone, the confining pressure may compress these areas and prevent moving CO_2-bearing fluids within the cement. Albeit this process also depends on other parameters such as the acidity, the brine composition, the confining pressure, the pore pressure, and the residence time.

The high-quality assemblage of a rock-cement-casing can provide a good barrier in preventing CO_2 from leaking upwards [11,45]. Otherwise, any defects in bonding between the cement and casing or cement and rock produces microannuluses which are highly conductive to CO_2 leakage [72].

No criterion is provided for evaluating the strength of cement-rock bonding. In addition, cement-rock bonding is not completely in a smooth cylindrical shape as assumed in most studies. During drilling mud filtrate pushes through the formation surrounding the well resulting in an alteration in brine composition. The presence of mud cake on the surface of the formation or caprock generally negatively affects the bonding between the rock and cement.

Although many efforts have been conducted on the geomechanical characterization of cement behaviour exposed to CO_2-bearing fluids, more detailed investigation is required to import the change in geomechanical properties of cement and rock during CO_2 exposure into modelling formulations. Outstanding aspects that contribute to either self-sealing or opening behaviour of the cement alteration process are as follows: fluid pressure, confining pressure, crystallization pressure (due to crystallization of precipitated calcium carbonate), changes in mechanical properties of altered zones and asperities or pillars in fracture, movement of separated particles along fractures and gaps, and swelling amorphous silica gel layer. There is a need to incorporate these parameters in further modelling studies. Different types of additives are used to change the properties of cement to match required special conditions at different depths when the well was cemented.

Many abandoned wells have been cemented using modified cements by additives, therefore the chemical and physical properties of cured cement to a great extent is influenced by the presence of additives such as accelerators, retarders, extenders, fluid loss and loss circulation additives, and dispersants. All of these factors need to be considered in modelling the cement alteration exposed to CO_2-bearing fluids. Having reviewed well cements in the presence of CO_2, recommendations for future works include a systematic experimental tests to investigate the effect of different additives used in a single well. This will help CCS community to have a better understanding of the well integrity in case CO_2 leaks from the storage formation through wellbore when different additives were used while the well was cemented.

Acknowledgments

We would like to thank the staff at the Research Centre for Flow Measurement and Fluid Mechanics and the Centre for Built and Natural Environment at Coventry University for supporting us in developing this review by providing constructive comments and improving the manuscript. The authors also appreciates both centres at Coventry University for their financial support.

References

[1] T.F. Stocker, G.-K. Plattner, M.M.B. Tignor, S.K. Allen, J. Boschung, A. Nauels, Y. Xia, V. Bex, P.M. Midgley, Climate Change 2013, 2013. doi:10.1017/CBO9781107415324.Summary.

[2] J.T. Kiehl, K.E. Trenberth, Earth's Annual Global Mean Energy Budget, Bull. Am. Meteorol. Soc. 78 (1997) 5. doi:10.1175/1520-0477(1997)078<0197:EAGMEB>2.0.CO;2.

[3] Windows to the Universe, The Greenhouse Effect & Greenhouse Gases, (2007). https://www.windows2universe.org/earth/climate/greenhouse_effect_gases.html (accessed December 21, 2017).

[4] J.W. Carey, M. Wigand, S.J. Chipera, G. WoldeGabriel, R. Pawar, P.C. Lichtner, S.C. Wehner, M.A. Raines, G.D. Guthrie, Analysis and performance of oil well cement with 30 years of CO_2 exposure from the SACROC Unit, West Texas, USA, Int. J. Greenh. Gas Control. 1 (2007) 75–85. doi:10.1016/S1750-5836(06)00004-1.

[5] T.L. Watson, S. Bachu, Evaluation of the Potential for Gas and CO_2 Leakage Along Wellbores, E&P Environ. Saf. Conf. (2007) 115–126. doi:10.2118/106817-MS.

[6] T.L. Watson, S. Bachu, Identification of Wells with High CO_2-Leakage Potential in Mature Oil Fields Developed for CO_2-Enhanced Oil Recovery, 2008 SPE Improv. Oil Recover. Symp. (2008) 10. doi:10.2118/112924-MS.

[7] S. Bachu, T.L. Watson, Review of failures for wells used for CO_2 and acid gas injection in Alberta, Canada, Energy Procedia. 1 (2009) 3531–3537. doi:10.1016/j.egypro.2009.02.146.

[8] J.P.L. Brunet, L. Li, Z.T. Karpyn, N.J. Huerta, Fracture opening or self-sealing: Critical residence time as a unifying parameter for cement- CO_2-brine interactions, Int. J. Greenh. Gas Control. 47 (2016) 25–37. doi:10.1016/j.ijggc.2016.01.024.

[9] H.E. Mason, W.L. Du Frane, S.D.C. Walsh, Z. Dai, S. Charnvanichborikarn, S.A. Carroll, Chemical and mechanical properties of wellbore cement altered by CO_2-rich brine using a multianalytical approach, Environ. Sci. Technol. 47 (2013) 1745–1752. doi:10.1021/es3039906.

[10] S.D.C. Walsh, H.E. Mason, W.L. Du Frane, S.A. Carroll, Mechanical and hydraulic coupling in cement-caprock interfaces exposed to carbonated brine, Int. J. Greenh. Gas Control. 25 (2014) 109–120. doi:10.1016/j.ijggc.2014.04.001.

[11] S. Bachu, D.B. Bennion, Experimental assessment of brine and/or CO_2 leakage through well cements at reservoir conditions, Int. J. Greenh. Gas Control. 3 (2009) 494–501.

1048 doi:10.1016/j.ijggc.2008.11.002.

1049 [12] J.W. Carey, R. Svec, R. Grigg, J. Zhang, W. Crow, Experimental investigation of wellbore
1050 integrity and CO_2-brine flow along the casing-cement microannulus, Int. J. Greenh. Gas Control.
1051 4 (2010) 272–282. doi:10.1016/j.ijggc.2009.09.018.

1052 [13] L. Deremble, M. Loizzo, B. Huet, B. Lecampion, D. Quesada, Stability of a leakage pathway in
1053 a cemented annulus, Energy Procedia. 4 (2011) 5283–5290. doi:10.1016/j.egypro.2011.02.508.

1054 [14] N.J. Huerta, M.A. Hesse, S.L. Bryant, B.R. Strazisar, C.L. Lopano, Experimental evidence for
1055 self-limiting reactive flow through a fractured cement core: Implications for time-dependent
1056 wellbore leakage, Environ. Sci. Technol. 47 (2013) 269–275. doi:10.1021/es3013003.

1057 [15] J. Iyer, S.D.C. Walsh, Y. Hao, S.A. Carroll, Incorporating reaction-rate dependence in reaction-
1058 front models of wellbore-cement/carbonated-brine systems, Int. J. Greenh. Gas Control. 59
1059 (2017) 160–171. doi:10.1016/j.ijggc.2017.01.019.

1060 [16] V. Barlet-Gouédard, G. Rimmelé, B. Goffé, O. Porcherie, Well Technologies for CO_2 Geological
1061 Storage: CO_2-Resistant Cement, Oil Gas Sci. Technol. - Rev. l'IFP. 62 (2007) 325–334.
1062 doi:10.2516/ogst:2007027.

1063 [17] V. Barlet-Gouédard, G. Rimmelé, O. Porcherie, N. Quisel, J. Desroches, A solution against well
1064 cement degradation under CO_2 geological storage environment, Int. J. Greenh. Gas Control. 3
1065 (2009) 206–216. doi:10.1016/j.ijggc.2008.07.005.

1066 [18] G. Rimmelé, V. Barlet-Gouédard, O. Porcherie, B. Goffé, F. Brunet, Heterogeneous porosity
1067 distribution in Portland cement exposed to CO_2-rich fluids, Cem. Concr. Res. 38 (2008) 1038–
1068 1048. doi:10.1016/j.cemconres.2008.03.022.

1069 [19] Energy Institute, Good plant design and operation for onshore carbon capture installations and
1070 onshore pipelines, 44 (2010) 137.

1071 [20] N.N. Greenwood, A. Earnshaw, Chemistry of the elements, in: Elsevier, 2012: p. 310.

1072 [21] M.L. Druckenmiller, M.M. Maroto-Valer, Carbon sequestration using brine of adjusted pH to
1073 form mineral carbonates, Fuel Process. Technol. 86 (2005) 1599–1614.
1074 doi:10.1016/j.fuproc.2005.01.007.

1075 [22] R.K. Haghi, A. Chapoy, L.M.C. Peirera, J. Yang, B. Tohidi, pH of CO_2 saturated water and CO_2
1076 saturated brines: Experimental measurements and modelling, Int. J. Greenh. Gas Control. 66
1077 (2017) 190–203. doi:10.1016/j.ijggc.2017.10.001.

1078 [23] J.W. Carey, Geochemistry of Wellbore Integrity in CO_2 Sequestration: Portland Cement-Steel-
1079 Brine- CO_2 Interactions, Rev. Mineral. Geochemistry. 77 (2013) 505–539.
1080 doi:10.2138/rmg.2013.77.15.

1081 [24] M. Mainguy, F. Ulm, Coupled Diffusion-Dissolution Around a Fracture Channel : The Solute
1082 Congestion Phenomenon, Transp. Porous Media. 45 (2001) 481–497.
1083 doi:10.1023/A:1012096014084.

1084 [25] B.G. Kutchko, B.R. Strazisar, D.A. Dzombak, G. V Lowry, N. Thaulow, Degradation of Well
1085 Cement by CO_2 under Geological Sequestration Conditions, Env. Sci Technol. 41 (2007) 4787–
1086 4792. doi:10.1021/es062828c.

1087 [26] B.M. Huet, J.H. Prevost, G.W. Scherer, Quantitative reactive transport modeling of Portland
1088 cement in CO_2-saturated water, Int. J. Greenh. Gas Control. 4 (2010) 561–574.
1089 doi:10.1016/j.ijggc.2009.11.003.

1090 [27] A. Duguid, G.W. Scherer, Degradation of oilwell cement due to exposure to carbonated brine,
1091 Int. J. Greenh. Gas Control. 4 (2010) 546–560. doi:10.1016/j.ijggc.2009.11.001.

1092 [28] P.E. Dijk, B. Berkowitz, Characterizing flow and transport in factures geological media: A
1093 review, Adv. Water Resour. 25 (1999) 861–884. doi:10.1016/S0309-1708(02)00042-8.

1094 [29] S.D.C. Walsh, W.L. Du Frane, H.E. Mason, S.A. Carroll, Permeability of wellbore-cement
1095 fractures following degradation by carbonated brine, Rock Mech. Rock Eng. 46 (2013) 455–464.
1096 doi:10.1007/s00603-012-0336-9.

1097 [30] H.F.W. Taylor, Cement chemistry, in: T. Telford, 1997: p. 123.

1098 [31] J. Shen, P. Dangla, M. Thiery, Reactive transport modeling of CO_2 through cementitious
1099 materials under CO_2 geological storage conditions, Int. J. Greenh. Gas Control. 18 (2013) 75–
1100 87. doi:10.1016/j.ijggc.2013.07.003.

1101 [32] J.J. Chen, J.J. Thomas, H.F.W. Taylor, H.M. Jennings, Solubility and structure of calcium silicate

hydrate, Cem. Concr. Res. 34 (2004) 1499–1519. doi:10.1016/J.CEMCONRES.2004.04.034.

[33] J. Liaudat, A. Martínez, C.M. López, I. Carol, Modelling acid attack of oilwell cement exposed to carbonated brine, Int. J. Greenh. Gas Control. 68 (2018) 191–202. doi:10.1016/j.ijggc.2017.11.015.

[34] A. Trapote-Barreira, J. Cama, J.M. Soler, Dissolution kinetics of C-S-H gel: Flow-through experiments, Phys. Chem. Earth. 70–71 (2014) 17–31. doi:10.1016/j.pce.2013.11.003.

[35] J. Corvisier, A. Fabbri, F. Brunet, Y. Leroy, B. Goffé, G. Rimmelé, V. Barlet-Gouédard, A Numerical Model for CO_2 Wells Ageing through Water/Supercritical CO_2/Cement Interactions, in: Thermo-Hydromechanical Chem. Coupling Geomaterials Appl., John Wiley & Sons, Inc., Hoboken, NJ, USA, 2013: pp. 75–84. doi:10.1002/9781118623565.ch5.

[36] E. Nourtier-Mazauric, B. Guy, B. Fritz, E. Brosse, D. Garcia, A. Clément, Modelling the Dissolution / Precipitation of Ideal Solid Solutions, Oil Gas Sci. Technol. - Rev. IFP. 60 (2005) 401–415. doi:10.2516/ogst:2005024.

[37] Z. Duan, R. Sun, An improved model calculating CO_2 solubility in pure water and aqueous NaCl solutions from 273 to 533 K and from 0 to 2000 bar, Chem. Geol. 193 (2003) 257–271. doi:10.1016/S0009-2541(02)00263-2.

[38] N. Spycher, K. Pruess, J. Ennis-King, CO_2-H_2O mixtures in the geological sequestration of CO_2. I. Assessment and calculation of mutual solubilities from 12 to 100°C and up to 600 bar, Geochim. Cosmochim. Acta. 67 (2003) 3015–3031. doi:10.1016/S0016-7037(03)00273-4.

[39] J. Gibbins, H. Chalmers, Carbon capture and storage, Energy Policy. 36 (2008) 4317–4322. doi:10.1016/j.enpol.2008.09.058.

[40] P. Córdoba, L. Cherqaoui, S. Garcia, M.M. Maroto-Valer, Effect of Limestone and Buffer Solution in the Aqueous Speciation and pH of Brines for CO_2 Sequestration, Energy Procedia. 114 (2017) 4865–4871. doi:10.1016/j.egypro.2017.03.1627.

[41] Q. Liu, M.M. Maroto-Valer, Investigation of the effect of brine composition and pH buffer on CO_2-brine sequestration, Energy Procedia. 4 (2011) 4503–4507. doi:10.1016/j.egypro.2011.02.406.

[42] ASTM D5084-03., Standard Test Methods for Measurement of Hydraulic Conductivity of Saturated Porous Materials Using a Flexible Wall Permeameter, Methods. (2010) 1–23. doi:10.1520/D5084-03.1.3.2.

[43] J. Corvisier, F. Brunet, A. Fabbri, S. Bernard, N. Findling, G. Rimmelé, V. Barlet-Gouédard, O. Beyssac, B. Goffé, Raman mapping and numerical simulation of calcium carbonates distribution in experimentally carbonated Portland-cement cores, Eur. J. Mineral. 22 (2010) 63–74. doi:10.1127/0935-1221/2010/0022-1977.

[44] B.G. Kutchko, B.R. Strazisar, N. Huerta, G. V. Lowry, D.A. Dzombak, N. Thaulow, CO_2 reaction with hydrated class H well cement under geologic sequestration conditions: Effects of flyash admixtures, Environ. Sci. Technol. 43 (2009) 3947–3952. doi:10.1021/es803007e.

[45] L. Zhang, D.A. Dzombak, D. V. Nakles, J.P.L. Brunet, L. Li, Reactive transport modeling of interactions between acid gas (CO_2 + H_2S) and pozzolan-amended wellbore cement under geologic carbon sequestration conditions, Energy and Fuels. 27 (2013) 6921–6937. doi:10.1021/ef401749x.

[46] P.A. Domenico, D.B. Harris, F.W. Schwartz, J. Wiley, Physical and Chemical Hydrogeology Second Edition, in: Wiley, 1998: p. 215.

[47] H. Abdoulghafour, P. Gouze, L. Luquot, R. Leprovost, Characterization and modeling of the alteration of fractured class-G Portland cement during flow of CO_2-rich brine, Int. J. Greenh. Gas Control. 48 (2016) 155–170. doi:10.1016/j.ijggc.2016.01.032.

[48] N.J. Huerta, M.A. Hesse, S.L. Bryant, B.R. Strazisar, C. Lopano, CO_2-saturated water in a cement fracture : Application to wellbore leakage during geologic CO_2 storage, 44 (2016) 276–289.

[49] B. Huet, R. Fuller, J. Prevost, Development of a coupled geochemical transport code to simulate cement degradation in CO_2 saturated brine, Eighth Int. Conf. Greenh. Gas Control Technol. June 19-22, 2006, Trondheim, Norw. (2006).

[50] N. Hyvert, A. Sellier, F. Duprat, P. Rougeau, P. Francisco, Dependency of C-S-H carbonation rate on CO_2 pressure to explain transition from accelerated tests to natural carbonation, Cem.

Concr. Res. 40 (2010) 1582–1589. doi:10.1016/j.cemconres.2010.06.010.

[51] C. Geloni, T. Giorgis, A. Battistelli, Modeling of Rocks and Cement Alteration due to CO_2 Injection in an Exploited Gas Reservoir, Transp. Porous Media. 90 (2011) 183–200. doi:10.1007/s11242-011-9714-0.

[52] J.H. Prévost, DYNAFLOW: A Nonlinear Transient Finite Element Analysis Program, Princeton University, 1981. https://www.princeton.edu/~dynaflow/.

[53] A. Duguid, Degradation of Well Cements Exposed to Carbonated Brine, Fourth Annu. Conf. Carbon Capture Sequestration Doe/Netl. (2005) 1–12.

[54] F.P. Wang, R.M. Reed, Pore Networks and Fluid Flow in Gas Shales, SPE Annu. SPE 124253 (2009) 8. doi:10.2118/124253-MS.

[55] B.G. Kutchko, B.R. Strazisar, G.V. Lowry, D. a. Dzombak, N. Thaulow, Rate of CO_2 Attack on Hydrated Class H Well Cement under Geologic Sequestration Conditions, Environ. Sci. \& Technol. 42 (2008) 6237–6242. doi:10.1021/es800049r.

[56] K. Pruess, Numerical Simulation of CO_2 Leakage From a Geologic Disposal Reservoir, Including Transitions From Super- to Subcritical Conditions, and Boiling of Liquid CO_2, SPE J. 9 (2004) 237–248. doi:10.2118/86098-PA.

[57] J.P.L. Brunet, L. Li, Z.T. Karpyn, B.G. Kutchko, B. Strazisar, G. Bromhal, Dynamic evolution of cement composition and transport properties under conditions relevant to geological carbon sequestration, Energy and Fuels. 27 (2013) 4208–4220. doi:10.1021/ef302023v.

[58] S. Carroll, J.W. Carey, D. Dzombak, N.J. Huerta, L. Li, T. Richard, W. Um, S.D.C. Walsh, L. Zhang, Review: Role of chemistry, mechanics, and transport on well integrity in CO_2 storage environments, Int. J. Greenh. Gas Control. 49 (2016) 149–160. doi:10.1016/j.ijggc.2016.01.010.

[59] G.W. Scherer, B. Huet, Carbonation of wellbore cement by CO_2 diffusion from caprock, Int. J. Greenh. Gas Control. 3 (2009) 731–735. doi:10.1016/j.ijggc.2009.08.002.

[60] A. Sauki, S. Irawan, Effects of Pressure and Temperature on Well Cement Degradation by Supercritical CO_2, Int. J. Eng. Technol. IJET-IJENS. 10 (2010) 53–61. http://eprints.utp.edu.my/4729/.

[61] B. Strazisar, B. Kutchko, N. Huerta, Chemical Reactions of Wellbore Cement Under CO_2 Storage Conditions: Effects of Cement Additives, Energy Procedia. 1 (2009) 3603–3607. doi:10.1016/j.egypro.2009.02.155.

[62] G. Rimmelé, V. Barlet-Gouédard, Accelerated degradation method for cement under CO_2-rich environment: The LIFTCO2 procedure (leaching induced by forced transport in CO_2 fluids), Cem. Concr. Res. 40 (2010) 1175–1188. doi:10.1016/j.cemconres.2010.03.019.

[63] M. Recasens, S. Garcia, E. Mackay, J. Delgado, M.M. Maroto-Valer, Experimental study of wellbore integrity for CO_2 geological storage, Energy Procedia. 114 (2017) 5249–5255. doi:10.1016/j.egypro.2017.03.1681.

[64] L. Luquot, H. Abdoulghafour, P. Gouze, Hydro-dynamically controlled alteration of fractured Portland cements flowed by CO_2-rich brine, Int. J. Greenh. Gas Control. 16 (2013) 167–179. doi:10.1016/j.ijggc.2013.04.002.

[65] Y. Asahara, S. Mito, Z. Xue, Y. Yamashita, K. Miyashiro, Chemical impacts of CO_2 flooding on well composite samples: Experimental assessment of well integrity for CO_2 sequestration, Energy Procedia. 37 (2013) 5738–5745. doi:10.1016/j.egypro.2013.06.496.

[66] P. Cao, Z.T. Karpyn, L. Li, Self-healing of cement fractures under dynamic flow of CO_2-rich brine, Water Resour. Res. 51 (2015) 4684–4701. doi:10.1002/2014WR016162.

[67] I. Falcon-Suarez, G. Papageorgiou, A. Chadwick, L. North, A.I. Best, M. Chapman, $CO_2$2-brine flow-through on an Utsira Sand core sample: Experimental and modelling. Implications for the Sleipner storage field, Int. J. Greenh. Gas Control. 68 (2018) 236–246. doi:10.1016/j.ijggc.2017.11.019.

[68] A. Akhavan, S.M.H. Shafaatian, F. Rajabipour, Quantifying the effects of crack width, tortuosity, and roughness on water permeability of cracked mortars, Cem. Concr. Res. 42 (2012) 313–320. doi:10.1016/j.cemconres.2011.10.002.

[69] G. Dávila, L. Luquot, J.M. Soler, J. Cama, 2D reactive transport modeling of the interaction between a marl and a CO_2-rich sulfate solution under supercritical CO_2 conditions, Int. J. Greenh. Gas Control. 54 (2016) 145–159. doi:10.1016/j.ijggc.2016.08.033.

1210 [70] A. Hernández-Rodríguez, G. Montegrossi, B. Huet, O. Vaselli, G. Virgili, A study of wellbore
1211 cement alteration controlled by CO_2 leakage in a natural analogue for geological CO_2 storage,
1212 Appl. Geochemistry. 86 (2017) 13–25. doi:10.1016/j.apgeochem.2017.09.010.

1213 [71] S.D.C. Walsh, H.E. Mason, W.L. Du Frane, S.A. Carroll, Experimental calibration of a
1214 numerical model describing the alteration of cement/caprock interfaces by carbonated brine, Int.
1215 J. Greenh. Gas Control. 22 (2014) 176–188. doi:10.1016/j.ijggc.2014.01.004.

1216 [72] N.J. Huerta, S.L. Bryant, L. Conrad, Cement Core Experiments With A Conductive Leakage
1217 Pathway , Under Confining Stress And Alteration Of Cement ' s Mechanical Properties Via A
1218 Reactive Fluid , As An Analog For CO_2 Leakage Scenario, SPE/DOE Improv. Oil Recover.
1219 Symp. Tulsa, Oklahoma, 19-23 April. SPE-113375 (2008). doi:10.2118/113375-MS.

1220 [73] N.J. Huerta, S.L. Bryant, B.R. Strazisar, B.G. Kutchko, L.C. Conrad, The influence of confining
1221 stress and chemical alteration on conductive pathways within wellbore cement, Energy Procedia.
1222 1 (2009) 3571–3578. doi:10.1016/j.egypro.2009.02.151.

1223 [74] K. Nakano, S. Mito, Z. Xue, Self-sealing of Wellbore Cement under the CO_2 Batch Experiment
1224 Using Well Composite Sample, Energy Procedia. 114 (2017) 5212–5218.
1225 doi:10.1016/j.egypro.2017.03.1677.

1226 [75] A. Fabbri, J. Corvisier, A. Schubnel, F. Brunet, B. Goffé, G. Rimmele, V. Barlet-Gouédard,
1227 Effect of carbonation on the hydro-mechanical properties of Portland cements, Cem. Concr. Res.
1228 39 (2009) 1156–1163. doi:10.1016/j.cemconres.2009.07.028.

1229 [76] T. Xiao, B. McPherson, A. Bordelon, H. Viswanathan, Z. Dai, H. Tian, R. Esser, W. Jia, W.
1230 Carey, Quantification of CO_2-cement-rock interactions at the well-caprock-reservoir interface
1231 and implications for geological CO_2 storage, Int. J. Greenh. Gas Control. 63 (2017) 126–140.
1232 doi:10.1016/j.ijggc.2017.05.009.

1233 [77] M. Wigand, J.P. Kaszuba, J.W. Carey, W.K. Hollis, Geochemical effects of CO_2 sequestration
1234 on fractured wellbore cement at the cement/caprock interface, Chem. Geol. 265 (2009) 122–133.
1235 doi:10.1016/j.chemgeo.2009.04.008.

1236 [78] J. Han, J.W. Carey, J. Zhang, A coupled electrochemical-geochemical model of corrosion for

1237 mild steel in high-pressure CO_2-saline environments, Int. J. Greenh. Gas Control. 5 (2011) 777–
1238 787. doi:10.1016/j.ijggc.2011.02.005.

1239 [79] J. Han, J. Zhang, J.W. Carey, Effect of bicarbonate on corrosion of carbon steel in CO_2 saturated
1240 brines, Int. J. Greenh. Gas Control. 5 (2011) 1680–1683. doi:10.1016/j.ijggc.2011.08.003.

1241 [80] S.M. Shariatipour, G.E. Pickup, E.J. Mackay, The Effect of Aquifer/Caprock Interface on
1242 Geological Storage of CO_2, Energy Procedia. 63 (2014) 5544–5555.
1243 doi:10.1016/J.EGYPRO.2014.11.588.

1244 [81] S.M. Shariatipour, G.E. Pickup, E.J. Mackay, Simulations of CO_2 storage in aquifer models with
1245 top surface morphology and transition zones, Int. J. Greenh. Gas Control. 54 (2016) 117–128.
1246 doi:10.1016/J.IJGGC.2016.06.016.

1247 [82] M.M. Smith, Y. Sholokhova, Y. Hao, S.A. Carroll, Evaporite caprock integrity: An experimental
1248 study of reactive mineralogy and pore-scale heterogeneity during brine- CO_2 exposure, Environ.
1249 Sci. Technol. 47 (2013) 262–268. doi:10.1021/es3012723.

1250 [83] M. Zhang, S. Bachu, Review of integrity of existing wells in relation to CO_2 geological storage:
1251 What do we know?, Int. J. Greenh. Gas Control. 5 (2011) 826–840.
1252 doi:10.1016/j.ijggc.2010.11.006.

1253 [84] W.W. McNab, S.A. Carroll, Wellbore integrity at the Krechba carbon storage site, In Salah,
1254 Algeria: 2. Reactive transport modeling of geochemical interactions near the cement-formation
1255 interface, Energy Procedia. 4 (2011) 5195–5202. doi:10.1016/j.egypro.2011.02.497.

1256 [85] A. Duguid, M. Radonjic, G.W. Scherer, Degradation of cement at the reservoir/cement interface
1257 from exposure to carbonated brine, Int. J. Greenh. Gas Control. 5 (2011) 1413–1428.
1258 doi:10.1016/j.ijggc.2011.06.007.

1259 [86] T.J. Wolery, R.L. Jarek, Software user's manual EQ3/6, (Version 8.0), 2003.

1260 [87] L. Connell, D. Down, M. Lu, D. Hay, D. Heryanto, An investigation into the integrity of wellbore
1261 cement in CO_2 storage wells: Core flooding experiments and simulations, Int. J. Greenh. Gas
1262 Control. 37 (2015) 424–440. doi:10.1016/j.ijggc.2015.03.038.

1263 [88] A. Nagelhout, M.G.R. Bosma, P. Mul, G. Krol, H. van Velzen, J. Joldersma, S.G. James, B.

Dargaud, R. Schreuder, F. Thery, Laboratory and Field Validation of Cement Systems for Critical Plug-and-Abandon Applications, SPE/IADC Middle East Drill. Technol. Conf. Exhib. (2005). doi:10.2118/97347-MS.

[89] R. Marlow, Cement Bonding Characteristics in Gas Wells, J. Pet. Technol. 41 (1989) 1146–1153. doi:10.2118/17121-PA.

[90] K.J. Goodwin, R.J. Crook, Cement Sheath Stress Failure, SPE Drill. Eng. 7 (1992) 291–296. doi:10.2118/20453-PA.

[91] H.A. Nasr-El-Din, Y.A. Elmarsafawi, A.S. Al-Yami, A Study of Acid Cement Reactions Using the Rotating Disk Apparatus, in: Int. Symp. Oilf. Chem., Society of Petroleum Engineers, 2007. doi:10.2118/106443-MS.

[92] F.J. Ulm, E. Lemarchand, F.H. Heukamp, Elements of chemomechanics of calcium leaching of cement-based materials at different scales, Eng. Fract. Mech. 70 (2003) 871–889. doi:10.1016/S0013-7944(02)00155-8.

[93] O. Coussy, F.-J. Ulm, Creep and plasticity due to chemo-mechanical couplings, Arch. Appl. Mech. 66 (1996) 523–535. doi:10.1007/BF00808142.

[94] B. Lecampion, J. Vanzo, F.-J. Ulm, B. Huet, C. Germay, I. Khalfallah, J. Dirrenberger, Evolution of Portland Cement Mechanical Properties Exposed To CO_2-Rich Fluids: Investigation At Different Scales, MPPS 2011, Symp. Mech. Phys. Porous Solids A Tribut. to Pr. Oliv. Coussy. (2011) 1–24.

[95] J.K. Fink, Petroleum engineer's guide to oil field chemicals and fluids, in: Gulf Professional Pub, 2012: pp. 312–317.

[96] E.B. Nelson, Well cementing, in: Elsevier, 1990: pp. 28–44.

[97] K.L. Scrivener, P. Juilland, P.J.M. Monteiro, Advances in understanding hydration of Portland cement, Cem. Concr. Res. 78 (2015) 38–56. doi:10.1016/j.cemconres.2015.05.025.

[98] The National Institute of Standards and Technology (NIST), Cement Hydration and Degradation Modeling Software, (2017). https://www.nist.gov/el/materials-and-structural-systems-division-73100/inorganic-materials-group-73103/concretenistgov (accessed February 19, 2018).

[99] R.H. Bogue, W. Lerch, Hydration of Portland Cement Compounds, Ind. Eng. Chem. 26 (1934) 837–847. doi:10.1021/ie50296a007.

[100] P.T. Durdziński, M. Ben Haha, M. Zajac, K.L. Scrivener, Phase assemblage of composite cements, Cem. Concr. Res. 99 (2017) 172–182. doi:10.1016/j.cemconres.2017.05.009.

[101] C. Hall, K.L. Scrivener, Oilwell cement clinkers x-ray microanalysis and phase composition, Adv. Cem. Based Mater. 7 (1998) 28–38. doi:10.1016/S1065-7355(97)00035-7.

[102] R. Jacob, B.Z. Saylor, CO_2 solubility in multi-component brines containing NaCl, KCl, $CaCl_2$ and $MgCl_2$ at 297 K and 1-14 MPa, Chem. Geol. 424 (2016) 86–95. doi:10.1016/j.chemgeo.2016.01.013.

[103] P.C. Aïtcin, Cements of yesterday and today - concrete of tomorrow, Cem. Concr. Res. 30 (2000) 1349–1359. doi:10.1016/S0008-8846(00)00365-3.

[104] B. Huet, V. Tasoti, I. Khalfallah, A review of Portland cement carbonation mechanisms in CO_2 rich environment, Energy Procedia. 4 (2011) 5275–5282. doi:10.1016/j.egypro.2011.02.507.

[105] A. Raoof, H.M. Nick, T.K.T. Wolterbeek, C.J. Spiers, Pore-scale modeling of reactive transport in wellbore cement under CO_2 storage conditions, Int. J. Greenh. Gas Control. 11 (2012) 67–77. doi:10.1016/j.ijggc.2012.09.012.

[106] F. Gherardi, P. Audigane, E.C. Gaucher, Predicting long-term geochemical alteration of wellbore cement in a generic geological CO_2 confinement site: Tackling a difficult reactive transport modeling challenge, J. Hydrol. 420–421 (2012) 340–359. doi:10.1016/j.jhydrol.2011.12.026.

[107] J. Iyer, S.D.C. Walsh, Y. Hao, S.A. Carroll, Assessment of two-phase flow on the chemical alteration and sealing of leakage pathways in cemented wellbores, Int. J. Greenh. Gas Control. 69 (2018) 72–80. doi:10.1016/j.ijggc.2017.12.001.

[108] L. Urbonas, V. Leno, D. Heinz, Effect of carbonation in supercritical CO_2 on the properties of hardened cement paste of different alkalinity, Constr. Build. Mater. 123 (2016) 704–711. doi:10.1016/j.conbuildmat.2016.07.040.

[109] O. Omosebi, H. Maheshwari, R. Ahmed, S. Shah, S. Osisanya, S. Hassani, G. DeBruijn, W. Cornell, D. Simon, Degradation of well cement in HPHT acidic environment: Effects of CO_2

concentration and pressure, Cem. Concr. Compos. 74 (2016) 54–70. doi:10.1016/j.cemconcomp.2016.09.006.

[110] C.I. Steefel, C.A.J. Appelo, B. Arora, D. Jacques, T. Kalbacher, O. Kolditz, V. Lagneau, P.C. Lichtner, K.U. Mayer, J.C.L. Meeussen, S. Molins, D. Moulton, H. Shao, J. Šimůnek, N. Spycher, S.B. Yabusaki, G.T. Yeh, Reactive transport codes for subsurface environmental simulation, 2015. doi:10.1007/s10596-014-9443-x.